Characterization of the Second Metal Site on Avian Phosphoenolpyruvate Carboxykinase†

John J. Hlavaty‡ and Thomas Nowak*

Department of Chemistry and Biochemistry, Nieuwland Science Hall, University of Notre Dame, Notre Dame, Indiana 46556

Received July 22, 1999; Revised Manuscript Received November 24, 1999

ABSTRACT: Chicken liver phosphoenolpyruvate carboxykinase (PEPCK) requires two divalent cations for activity. One cation activates the enzyme through a direct interaction with the protein at site n_1. The second cation, at site n_2, acts in the cation−nucleotide complex that serves as a substrate. The Co^{3+}-(n_1)−PEPCK and Cr^{3+}(n_1)−PEPCK complexes were used to examine the kinetic, mechanistic, and binding properties of the n_2 metal. EPR studies performed on the Co^{3+}(n_1)−PEPCK−GTP complex yielded a stoichiometry of 1 mol of Mn^{2+} bound per mole of Co^{3+}(n_1)−PEPCK−GTP with a K_D of 5 μM. PRR studies show a significant enhancement for the Co^{3+}(n_1)−PEPCK−Mn^{2+}(n_2)−GDP complex. A change in enhancement in the presence of PEP suggests that PEP interacts with the second metal ion. The distance between Mn^{2+} at site n_2 on PEPCK and the cis and trans protons and the ^{31}P of PEP are 7.0, 7.5, and 4.8 Å, respectively, as measured by high-resolution NMR. PRR studies of the Co^{3+}(n_1)−PEPCK−Mn^{2+}-(n_2)−GTP and Co^{3+}(n_1)−PEPCK−Mn^{2+}(n_2)−GDP complexes as a function of frequency (ω_I) were used to estimate the hydration number of the n_2 metal to be between 0.5 and 0.7. The metal−metal distance for the M(n_1)−PEPCK−M(n_2)−GTP complex is approximately 8.3 Å, and the distance for the M(n_1)−PEPCK−M(n_2)−GDP complex is 9.2 Å. The change in the metal−metal distance suggests a conformational change at the active site of PEPCK occurs during catalysis. The Co^{3+}(n_1)−PEPCK complex was incubated with Co^{2+}, GTP, and H_2O_2 to create a doubly labeled and inactive Co^{3+}(n_1)−PEPCK−Co^{3+}(n_2)−GTP complex. The Co^{3+}(n_1)−PEPCK−Co^{3+}(n_2)−GTP complex was digested by LysC, and two cobalt-containing peptides were purified using RP-HPLC. Amino acid sequencing of the second cobalt-containing peptide points to the region of Tyr57−Lys76 of PEPCK. Asp66, Asp69, and Glu74 are all feasible ligands to the site n_2 metal.

Chicken liver mitochondrial phosphoenolpyruvate carboxykinase (EC 4.1.1.32) is a 67 kDa monomeric enzyme that catalyzes the reversible GTP[1] (ITP)-dependent conversion of OAA to PEP, GDP, and CO_2 (*1*). PEPCK functions as the committed step in gluconeogenesis.

$$\text{OAA} + \text{GTP (ITP)} \rightleftarrows \text{PEP} + \text{CO}_2 + \text{GDP (IDP)} \quad (1)$$

The protein sequence of the mature form of the mitochondrial isoenzyme of PEPCK from chicken liver has been derived from cDNA clones (*2*). X-ray crystallographic analysis of PEPCK has not been possible due to the inability to crystallize the eukaryotic form of the enzyme. A recent diffraction study of crystals of the *Escherichia coli* PEPCK has been reported (*3*). Little sequence homology exists between the *E. coli* and chicken liver mitochondrial enzymes. Ca^{2+} is the best activator for *E. coli* PEPCK but a poor activating cation for the chicken liver mitochondrial PEPCK (<10% of that of Mn^{2+}). *E. coli* PEPCK is an ATP-dependent kinase, while avian liver PEPCK uses GTP and neither is activated by nor binds to ATP. The information that can be extracted from the *E. coli* PEPCK three-dimensional structure and applied to the chicken liver mitochondrial PEPCK is limited.

PEPCK shows an absolute requirement for divalent cations for activity, and Mn^{2+} is the best activator for chicken liver mitochondrial PEPCK. Mixed metal studies showed a dual cation role for PEPCK (*4*). One metal is associated with the enzyme, while the other is complexed to the nucleotide. The metal−nucleotide complex serves as the substrate. The first metal site, represented as n_1, is the binding site for the metal

† Research supported by NIH Grant DK17049 to T.N. and the Graduate Assistance in Areas of National Needs Program Fellowship (Project Award P200A20261) to J.J.H.

* To whom correspondence should be addressed. E-mail: Nowak.1@nd.edu. Telephone: (219) 631-5859.

‡ Present address: New England BioLabs, 32 Tozer Rd., Beverly, MA 01915.

[1] Abbreviations: AA, atomic absorption; β-met, 2-mercaptoethanol; CE, capillary electrophoresis; Co^{3+}−GDP, $Co(NH_3)_4GDP$; Co^{3+}−GTP, $Co(NH_3)_4GTP$; Cr^{3+}−GDP, $Cr(H_2O)_4GDP$; Cr^{3+}−GTP, $Cr(H_2O)_4GTP$; Co^{3+}(n_1)−PEPCK, PEPCK modified with Co^{3+} at metal site n_1; Co^{3+}-(n_1)−PEPCK−Co^{3+}(n_2)−GTP, PEPCK labeled at both metal sites; Cr^{3+}-(n_1)−PEPCK, PEPCK modified with Cr^{3+} at metal site n_1; DEAE, diethylaminoethyl; DTNB, 5,5′-dithiobis(2-nitrobenzoic acid); EDTA, ethylenediaminetetraacetic acid; EPR, electron paramagnetic resonance; GDP, guanosine 5′-diphosphate; GTP, guanosine 5′-triphosphate; HPLC, high-performance liquid chromatography; NAD^+, nicotinamide adenine dinucleotide; NADH, reduced nicotinamide adenine dinucleotide; NDP, nucleoside 5′-diphosphate; OAA, oxaloacetate; PEP, phosphoenolpyruvate; PEPCK, phosphoenolpyruvate carboxykinase; PRR, water proton longitudinal relaxation rate; Tris, tris(hydroxymethyl)aminoethane.

10.1021/bi991692a CCC: $19.00
Published on Web 01/20/2000

that directly interacts with the enzyme. The second metal site, represented as n_2, is the binding site for the metal that interacts with the nucleotide.

The binding of Mn^{2+} at site n_1 activates PEP for phosphoryl transfer to the nucleotide, but it is not directly involved in the carboxylation process. From ^1H and ^{31}P NMR studies, the substrates form Michaelis complexes in the outer sphere of the PEPCK-bound Mn^{2+} at site n_1 (*5*, *6*). Frequency-dependent PRR studies suggest that two water ligands are associated with the Mn^{2+} at site n_1, indicating that the enzyme provides four ligands to the hexacoordinate metal (*5*). At least one of these water molecules on the Mn^{2+} serves as a bridge between the substrate and enzyme-bound metal. Two amino acids associated with n_1 metal binding site were identified as Asp295 and Asp296 (*7*, *8*). Crystallographic analysis of the *E. coli* PEPCK (*3*) revealed that Asp269 was directly coordinated to the active site metal. Asp269 from the *E. coli* enzyme corresponds to Asp296 in avian liver PEPCK. While the overall homology between *E. coli* PEPCK and chicken liver mitochondrial PEPCK is poor, the metal binding site appears to be conserved. The PEPCK ligands, if any, for the n_2 metal site are unknown.

The role of the second metal is less clear. Lee et al. (*9*) proposed that the n_2 metal is in a β,γ-bidentate coordination with GTP. This proposal was based on the lack of any significant dependence of stereoselectivity of thiophosphate derivatives of GTP on the second metal ion. No interaction of the n_2 metal with the α-thiophosphate group of GTP or GDP was indicated. The second metal activates the γ-phosphoryl moiety of GTP, facilitating the nucleophilic attack by the substrate OAA. In the reverse direction, the second cation interacts with the β-phosphate of GDP and may stabilize the product GTP, making the phosphoryl group from the substrate PEP a better leaving group. The role of the second metal may also be to elicit the proper conformation of GDP and of GTP that is necessary during catalysis.

Recently, active $Co^{3+}(n_1)$−PEPCK (*7*) and $Cr^{3+}(n_1)$−PEPCK (*10*) complexes have been synthesized. The exchange-inert properties of Co^{3+} and Cr^{3+} complexes allowed PEPCK to be chemically modified at the n_1 metal binding site. The $Co^{3+}(n_1)$−PEPCK and $Cr^{3+}(n_1)$−PEPCK complexes provide excellent tools for examining the kinetic, mechanistic, and binding properties of the n_2 metal without the concern of additional metal binding equilibria at site n_1. Balakrishnan and Villafranca (*11*) showed that by using Co^{3+}- and Cr^{3+}-modified glutamine synthetase, the distance between the enzyme-bound metal and the metal associated with the nucleotide was estimated to be 7 ± 2 Å. The $Co^{3+}(n_1)$−glutamine synthetase complex served as a diamagnetic control. Binding studies with the $Co^{3+}(n_1)$−PEPCK−GTP or −GDP complexes revealed a second metal binding site, n_2. The same principles utilized for the modified glutamine synthetase complexes were applied to PEPCK. By using PRR techniques, the distance between the two paramagnetic metal ion centers in the $Cr^{3+}(n_1)$−PEPCK−$Mn^{2+}(n_2)$−GTP or −GDP complex was estimated.

Kramer and Nowak (*12*) showed that Cr^{3+}−GTP and Co^{3+}−GTP complexes are good competitive inhibitors of PEPCK, indicating that these nucleotide analogues interact at the active site of PEPCK. In the work presented here, we utilized both Cr^{3+}−GTP and Co^{3+}−GTP along with the $Co^{3+}(n_1)$−PEPCK and $Cr^{3+}(n_1)$−PEPCK complexes to gain additional information about the active site of PEPCK. In the absence of a three-dimensional X-ray crystal structure for avian liver mitochondrial PEPCK, the distance information obtained from the modified enzyme and nucleotide complexes, combined with previously obtained distance estimates, provides a three-dimensional view of the PEPCK active site.

The protein ligands for the second metal site were determined using a novel technique not previously reported. A doubly labeled PEPCK complex was formed when $Co^{3+}(n_1)$−PEPCK was treated with Co^{2+}, GTP, and H_2O_2 to create a $Co^{3+}(n_1)$−PEPCK−$Co^{3+}(n_2)$−GTP complex. This second Co^{3+} metal ion is associated with the nucleotide as well as the enzyme. This paper discusses the formation and properties of this doubly labeled enzyme complex and the identification of the protein ligands for the second metal.

MATERIALS AND METHODS

Materials. Malate dehydrogenase, LysC, pyruvate kinase, and lactate dehydrogenase were purchased from Boehringer Mannheim Corp. GTP, ITP, GDP, IDP, PEP, OAA, NADH, $CaCl_2$, and tetramethylammonium sulfate were purchased from Sigma. $CoCl_2$, $CrCl_3$, and Tris base were purchased from Mallinckrodt. $MnCl_2$ and $MgCl_2$ were from Baker. Chelex-100, Dowex 50W-X2, DEAE-Sepharose, and hydroxyapatite A resin were from Bio-Rad. Butyl Sepharose was purchased from Pharmacia. $[Co(NH_3)_4CO_3]NO_3^+$ was a kind gift from G. Lappin at the University of Notre Dame. All other reagents were of the highest purity commercially available. All nonmetal solutions were passed through a Chelex-100 column to remove any contaminating metal ions. Metal solutions were prepared with distilled water which was passed through a mixed-bed deionizing column and then through a Chelex-100 column and adjusted to pH 4.0.

PEPCK Purification. Chicken liver mitochondrial PEPCK was purified by a modification of the procedure of Lee and Nowak (*5*) as reported by Hlavaty and Nowak (*7*). The enzyme used for all studies typically had a specific activity between 4.5 and 7 units/mg and was >95% pure.

PEPCK Assay. The PEPCK-catalyzed reaction of PEP carboxylation to OAA was assayed by the method of Noce and Utter (*13*) as modified by Hebda and Nowak (*14*). In this continuous assay, PEPCK activity was coupled to malate dehydrogenase and the oxidation of NADH was spectrophotometrically measured at 340 nm and 25 °C using a temperature-controlled cell. The specific activity is defined as the units of enzyme activity per milligram of protein where 1 unit is the amount of enzyme catalyzing the formation of 1 μmol of product per milliliter per minute under experimental conditions. The PEPCK-catalyzed reaction of OAA decarboxylation to pyruvate was assayed to determine if the $Co^{3+}(n_1)$−PEPCK−$Co^{3+}(n_2)$−GTP complex was catalytically active. PEPCK activity was coupled to pyruvate kinase and lactate dehydrogenase, and the oxidation of NADH was spectrophotometrically measured at 340 nm. All activity assays were performed with a Gilford 240 or 250 spectrometer. Kinetic data were treated with the "EZ-FIT" program, version 2.02, by Perrella Scientific Inc. (1989).

Substrate Concentration. When an accurate determination of the substrate concentration was required, such determinations were performed enzymatically. The concentration of

substrate was determined as the limiting reagent in the PEPCK assay described above. Metal solution concentrations were determined by AA.

Cobalt(III) Modification of the First Metal Site on PEPCK. The $Co^{3+}(n_1)$−PEPCK complex was prepared by the method of Hlavaty and Nowak (*7*). This procedure consistently gives 1:1 Co^{3+}:PEPCK ratios. The $Co^{3+}(n_1)$−PEPCK complex is stable at 4 °C for approximately 1 week with no loss of the Co^{3+} label or change in activity.

Chromium(III) Modification of the First Metal Site on PEPCK. The $Cr^{3+}(n_1)$−PEPCK complex was prepared starting with $CrCl_3$ as described by Hlavaty and Nowak (*10*). This procedure consistently provides 1:1 Cr^{3+}:PEPCK ratios. The $Cr^{3+}(n_1)$−PEPCK complex is stable for at least 3 days at 4 °C with no loss of the Cr^{3+} label or change in activity.

Preparation of $Co^{3+}(n_1)$−PEPCK−$Co^{3+}(n_2)$−GTP. The $Co^{3+}(n_1)$−PEPCK complex was prepared as described above (*7*). GTP (2 mM) and $CoCl_2$ (4 mM) were added to a 110 μM solution of the $Co^{3+}(n_1)$−PEPCK complex. The solution was allowed to equilibrate on ice for 30 min followed by the addition of 20 mM H_2O_2. H_2O_2 (20 mM) was also added to the $Co^{3+}(n_1)$−PEPCK complex as a control to determine if any oxidative damage to the $Co^{3+}(n_1)$−PEPCK complex occurred during this second modification process. The solutions were allowed to sit on ice for an additional 60 min with periodic gentle shaking. After incubation, the solutions were passed through a P6-DG (1 cm × 10 cm) column having a 1 cm layer of Chelex-100 on top equilibrated in 50 mM Tris-HCl buffer (pH 7.4). The modified enzyme was collected from the column and concentrated using a mini-Amicon concentrator with a PM30 membrane. The enzyme was assayed for protein concentration by Bradford assays, for cobalt concentration by AA, and for catalytic activity. UV measurements of standards and of the sample at 260 nm were used to determine the GTP:PEPCK stoichiometry. The doubly labeled enzyme complex was used immediately after preparation, as it would precipitate after approximately 24 h at 4 °C.

Preparation of Co^{3+}−GDP and Co^{3+}−GTP. Co^{3+}−GTP $[Co(NH_3)_4GTP]$ and Co^{3+}−GDP $[Co(NH_3)_4GDP]$ were prepared following the procedure for Co^{3+}−ATP (*15*). The synthesis of Co^{3+}−GTP and Co^{3+}−GDP used the amine $[Co(NH_3)_4CO_3]NO_3^-$ as the starting material. The Co^{3+}−GTP and Co^{3+}−GDP concentrations were determined by measuring absorption at 260 nm with an extinction coefficient of 15.4 cm^{-1} mM^{-1}.

Preparation of Cr^{3+}−GDP and Cr^{3+}−GTP. Cr^{3+}−GTP $[Cr(H_2O)_4GTP]$ was prepared and purified following the procedure for Cr^{3+}−ATP (*16*, *17*). The Cr^{3+}−GTP concentration was determined by measuring absorption at 260 nm with an extinction coefficient of 15.4 cm^{-1} mM^{-1}. Cr^{3+}−GDP $[Cr(H_2O)_4GDP]$ was prepared following the procedure for Cr^{3+}−ADP (*18*). The concentration was determined as with Cr^{3+}−GTP.

Mn^{2+} Binding. The binding of Mn^{2+} to various modified PEPCK complexes was assessed by measuring the water proton relaxation rates (PRRs) using a Seimco-pulsed NMR spectrometer at 24.3 MHz using the Carr−Purcell (*19*) 180°−τ−90° sequence. The enhancement values were calculated from the paramagnetic effect of the longitudinal relaxation rates ($1/T_{1p}$). A more rigorous description of this technique has been presented elsewhere (*20*), and an outline of the method was recently presented (*7*).

Mn^{2+} binding to various PEPCK complexes was also studied using EPR following the method of Hebda and Nowak (*21*). Samples were drawn into 1 mm (inside diameter) quartz capillary tubes. The free Mn^{2+} concentration of each sample was measured using a Varian E-9 X-band EPR spectrometer at a frequency of 9.52 GHz. The binding of Mn^{2+} to unmodified PEPCK was used as a control in all experiments. The number of binding sites and the binding constants were obtained from a Scatchard plot of the data (*22*) for both the PRR and EPR data.

The final concentration of enzyme samples was 50 μM. PRR and EPR measurements on the inactive or partially inactive enzyme samples were taken at room temperature. The enzyme samples were kept at pH 7.4.

Substrate Binding to $Co^{3+}(n_1)$−PEPCK−$Co^{3+}(n_2)$−GTP As Determined from Fluorescence. The binding of nucleotides to $Co^{3+}(n_1)$−PEPCK−$Co^{3+}(n_2)$−GTP was investigated by fluorescence. A computer-assisted SLM 8100 fluorescence spectrometer was used for all measurements. The sample cell holder was maintained at 24 °C using a circulating water bath. The $Co^{3+}(n_1)$−PEPCK−$Co^{3+}(n_2)$−GTP solution was prepared in 50 mM Tris-HCl buffer (pH 7.4) containing 100 mM KCl. Using a 1 mL quartz cell, the samples were separately measured at an excitation wavelength of 297 nm and an emission wavelength of 334 nm. At recorded time intervals, a known concentration of GTP or GDP was added directly into the quartz cell containing the enzyme solution. The amount of fluorescence quenching due to each addition of substrate was recorded.

Substrate Binding to the $Co^{3+}(n_1)$−PEPCK−$Mn^{2+}(n_2)$−GTP and $Co^{3+}(n_1)$−PEPCK−$Mn^{2+}(n_2)$−GDP Complexes As Determined from PRR Measurements. The binding of substrates to the $Co^{3+}(n_1)$−PEPCK−$Mn^{2+}(n_2)$−GTP or −GDP complexes was assessed by measuring the water proton relaxation rates (PRRs) using a Seimco-pulsed NMR spectrometer at 24.3 MHz using the Carr−Purcell (*19*) 180°−τ−90° sequence. The enhancement values were calculated from the paramagnetic effect of the longitudinal relaxation rates ($1/T_{1p}$).

In these studies, the metal is always the Mn^{2+} at the second metal site of PEPCK. The term ϵ^*, the observed enhancement for enzyme and paramagnetic metal in the presence of ligands, can be defined as follows:

$$\epsilon^* = \frac{[EM]_f}{[M]_t}\epsilon_b + \frac{[EMS]}{[M]_t}\epsilon_t \qquad (2)$$

[EM] and [EMS] are defined above and represent the concentrations of free $Co^{3+}(n_1)$−PEPCK−$Mn^{2+}(n_2)$−GTP or −GDP complexes and $Co^{3+}(n_1)$−PEPCK−$Mn^{2+}(n_2)$−GTP−substrate or −GDP−substrate complexes, respectively. The substrate is any titrant other than nucleotide. $[M]_t$ is the total Mn^{2+} concentration. The term ϵ_b is defined as the enhancement value when no additional substrate is present. In treatment of the data, $\epsilon_b = 7.0$ for the $Co^{3+}(n_1)$−PEPCK−$Mn^{2+}(n_2)$−GTP complex and $\epsilon_b = 4.2$ for the $Co^{3+}(n_1)$−PEPCK−$Mn^{2+}(n_2)$−GDP complex as determined from these

studies. The term ϵ_t is defined as the enhancement value at saturating substrate concentrations.

The enhancement values were measured as substrates were titrated into separate solutions of 100 μM Co^{3+}−PEPCK in 50 mM Tris-HCl (pH 7.4) with 100 mM KCl with 80 μM GTP or GDP and 70 μM Mn^{2+}. At these concentrations, approximately 90% of the Mn^{2+} was bound at site n_2. PRR measurements were taken at room temperature, and the enzyme samples were kept at pH 7.4.

The observed enhancements, ϵ*, are plotted versus substrate concentration, providing estimates for the values of K_3 and ϵ_t. K_3 represents the binding constant for the interaction of the substrate and the enzyme−metal complex as follows:

$$K_3 = \frac{[S]_f[EM]}{[EMS]} \tag{3}$$

where $[S]_f$ is the free substrate concentration, [EM] represents the concentration of the enzyme−metal complex [in this case the $Co^{3+}(n_1)$−PEPCK−$Mn^{2+}(n_2)$−nucleotide] not associated with the substrate, and [EMS] represents the concentration of the $Co^{3+}(n_1)$−PEPCK−$Mn^{2+}(n_2)$−nucleotide−substrate complex. The term ϵ_t is defined in eq 2. The titration curves were fit on the basis of eqs 2 and 3 using the computer program PRRFIT, written in Fortran. The program is designed using the least-squares method. The program generates values for K_3 and ϵ_t.

Second Metal Hydration Number. The hydration number for the second metal site was determined for the $Co^{3+}(n_1)$−PEPCK−$Mn^{2+}(n_2)$−GTP and −GDP complexes using PRR techniques. The procedure described by Hwang and Nowak (*23*) was followed. Longitudinal relaxation rates ($1/T_1$) of water protons (PRR) were measured with a Seimco-pulsed NMR spectrometer. The concentration of free Mn^{2+} in each sample was directly measured by EPR spectroscopy. After the PRR measurements, the samples were drawn into l mm quartz capillary tubes and the Mn^{2+} spectra were recorded on a Varian E-9 X-band EPR spectrometer.

The effects of frequency on $1/T_1$ for each complex were measured at 10.0, 13.5, 24.3, 35.3, and 45.3 MHz. The frequency was adjusted with a frequency synthesizer, and resonance was obtained by varying the magnetic field. Measurements were taken for each protein−nucleotide−metal complex at two different enzyme concentrations (80 and 90 μM). Normalized paramagnetic effects on the longitudinal relaxation rates, $1/pT_{1p}$, for the binary complex and the enzyme complexes are plotted as a function of the squared resonance frequency $(\omega_I)^2$. The effect of temperature on the $1/T_1$ of each complex was measured by passing cooled nitrogen over a thermostated heating filament before it arrived at the sample zone. The temperature was adjusted by heating the nitrogen. The temperature at the sample within the probe was measured directly by means of a thermocouple.

To calculate the hydration number, q, for Mn^{2+} in the various enzyme complexes, the correlation time τ_c must be known. The τ_c for the electron−nucleus interaction was estimated for each of the complexes that was studied utilizing the frequency dependence of the $1/pT_{1p}$ of water protons. The frequency-dependent data were fit on the basis of the Bloembergen−Morgan theory (*24*) using eqs 4−7 and by using the computer program FREQ, written in Table Curve, to simulate the data.

$$\frac{1}{pT_{1p}} = \frac{q}{T_{1M} + \tau_m} \tag{4}$$

$$\frac{1}{T_{1M}} = \frac{q[2S(S+1)\gamma^2 g^2 \beta^2]}{15r^6}\left(\frac{3\tau_c}{1+\omega_1{}^2\tau_c{}^2} + \frac{7\tau_c}{1+\omega_s{}^2\tau_c{}^2}\right) \tag{5}$$

$$\frac{1}{\tau_c} = \frac{1}{\tau_r} + \frac{1}{\tau_s} + \frac{1}{\tau_m} \tag{6}$$

$$\frac{1}{\tau_s} = B\frac{\tau_v}{1+\omega_s{}^2\tau_c{}^2} \tag{7}$$

The normalized relaxation rate ($1/pT_{1p}$) is directly proportional to the hydration number, q, and related to the relaxation time and residence time of the water (eq 4) (*25*). The relaxation rate ($1/T_{1M}$) is described by the simplified form of the Solomon−Bloembergen equation (eq 5) (*26*, *27*). S is the electron-spin quantum number. γ is the nuclear magnetogyric ratio. r is the ion−nuclear distance. g is the electronic "g" factor. β is the Bohr magneton. ω_I and ω_s are the Larmor angular precession frequencies for the nuclear and electron spins, respectively, where $\omega_s = 657\omega_I$. For these calculations, the rotational correlation time, τ_r, is approximated as the molecular mass of the species (67 000 Da) divided by 2000 (*28*). Details of this approach have been reviewed elsewhere (*23*). The program is designed using the least-squares method of solving all four equations simultaneously using an iterative fit. The program relates the normalized value of $1/pT_{1p}$ to the relaxation and to the water exchange rate. The values for the hydration number, q, and the correlation time, τ_c, are determined from the fit of the data.

Estimation of the Distance between the n_1 and n_2 Metal Sites on PEPCK. The distance between the enzyme-bound Mn^{2+} at site n_1 and Cr^{3+}−GTP at site n_2 or enzyme-bound Cr^{3+} at site n_1 and Mn^{2+}−GTP at site n_2 was investigated by PRR techniques. This process is described in detail by Gupta (*29*), who first utilized this PRR technique to determine the metal−metal distance on pyruvate kinase using Cr^{3+}−ATP and enzyme−Mn^{2+} (with Co^{3+}−ATP and enzyme−Mg^{2+} as diamagnetic controls). An outline of this method is described here.

Two paramagnetic metal ions with similar electron resonance frequencies may affect the relaxation properties of each other via concerted mutual spin flips, the process of cross-relaxation (*26*, *30*). The mutual cross-relaxation depends on the inverse 6th power of the distance between the spins, and the magnitude of the effect declines as the separation between the two paramagnetic centers is increased. The exchange of the spin magnetizations occurs due to the flip-flop terms (the $S_1{}^-S_2{}^+$ and $S_2{}^-S_1{}^+$ functions, where S_1 and S_2 denote the electron spin operators of the paramagnetic metals) of the dipolar interaction Hamiltonian. The concerted spin flips become the predominant mechanism for relaxation.

For this work, when one of the spins is Cr^{3+} as Cr^{3+}−GTP, it has an electron relaxation time (τ_s^{Cr}) much shorter than that of the other spin, Mn^{2+} (τ_s^{Mn}). Since the rotational correlation time of the entire molecule, τ_r, is long compared to τ_s^{Cr}, the cross-relaxation phenomenon shortens the effective spin−lattice relaxation time of the slowly relaxing spin (Mn^{2+} in this case) according to the following equation:

$$\left(\frac{1}{\tau_s^{Mn}}\right)_{Cr} - \left(\frac{1}{\tau_s^{Mn}}\right)_{Co} = \frac{2S^{Cr}(S^{Cr}+1)\gamma_{Cr}^{2}\gamma_{Mn}^{2}h^{2}}{15r^{6}}\left[\frac{\tau_s^{Cr}}{(1+\Delta\omega_s\tau_c^{Cr})^{2}}\right] \quad (8)$$

where S^{Cr} and τ_s^{Cr} are the net unpaired spin and the electron spin relaxation time of Cr^{3+}, respectively, γ_{Cr} and γ_{Mn} are the electronic gyromagnetic ratios for the Cr^{3+} and Mn^{2+} ions, respectively, and r is the $Mn^{2+}-Cr^{3+}$ distance. The term $(1/\tau_s^{Mn})_{Cr}$ is the electron spin−lattice relaxation rate of the slowly relaxing spin (Mn^{2+}) in the presence of the other paramagnetic spin (Cr^{3+}), and the term $(1/\tau_s^{Mn})_{Co}$ is the same quantity except that the faster relaxing spin is replaced by the diamagnetic metal, Co^{3+}. Co^{3+}−GTP provides a substitution-inert diamagnetic analogue for the paramagnetic Cr^{3+}−GTP. The combination of $Mn^{2+}(n_1)$−PEPCK−$Cr^{3+}(n_2)$−GTP and $Mn^{2+}(n_1)$−PEPCK−$Co^{3+}(n_2)$−GTP provides an excellent system for such a study. Both Co^{3+}−GTP and Cr^{3+}−GTP are inhibitors against and effectively replace Mg^{2+}−GTP at the active site of PEPCK (*12*).

The paramagnetic effect of Mn^{2+} on the longitudinal relaxation rate ($1/T_1$) of water protons is enhanced upon complexation with the enzyme. The relaxation times, τ_s^{Mn}, may be estimated from the observed enhancement factors for relaxation rates of the fast exchanging inner sphere water protons in appropriate systems. The observed enhancement ϵ^{Mn} of the Mn^{2+} relaxivity in the enzyme-bound form is related to the value of τ_c, where τ_c is the resultant correlation time of the process or processes responsible for the time dependence of the manganese−water proton dipolar interaction as demonstrated by the following equations:

$$\epsilon^{Mn} = \frac{qf(\tau_c)}{6\tau_r} \quad (9)$$

$$f(\tau_c) = \frac{3\tau_c}{1+\omega_I^{2}\tau_c^{2}} + \frac{7\tau_c}{1+\omega_s^{2}\tau_c^{2}} \quad (10)$$

where ω_I^2 is 2.33×10^{16} rad^2 s^2 (24.3 MHz), τ_r, the rotational correlation time for the hydrated Mn^{2+} ion, is 3×10^{-11} s, ω_I is the proton Larmor frequency, and ω_s is the Larmor frequency of the Mn^{2+} electronic spin moment. The number of fast exchanging water ligands of Mn^{2+} in the bound state is represented by q. For the hexaaquo complex of Mn^{2+}, $q = 6$ and $\tau_c = \tau_r = 3 \times 10^{-11}$ s.

To determine the distance between Mn^{2+} at site n_1 and Cr^{3+} at site n_2 in the $Mn^{2+}(n_1)$−PEPCK−$Cr^{3+}(n_2)$−GTP complex, the experiment consists of measuring the enhancements of the longitudinal relaxation rate of water protons in the $Mn^{2+}(n_1)$−PEPCK−$Cr^{3+}(n_2)$−GTP, $Mn^{2+}(n_1)$−PEPCK−$Co^{3+}(n_2)$−GTP, $Mg^{2+}(n_1)$−PEPCK−$Cr^{3+}(n_2)$−GTP, and $Mg^{2+}(n_1)$−PEPCK−$Co^{3+}(n_2)$−GTP complexes. The observed enhancement of the paramagnetic effect of Cr^{3+} on the water proton relaxation rate in the presence of the enzyme is small (1.5) compared to the much larger enhancement of the paramagnetic effect of Mn^{2+} (6−12). The small variation in the effect of Cr^{3+} on the water relaxation rates between $Mn^{2+}(n_1)$−PEPCK−$Cr^{3+}(n_2)$−GTP and $Mg^{2+}(n_1)$−PEPCK−$Cr^{3+}(n_2)$−GTP complexes due to the presence of cross-relaxations was neglected, and the much larger paramagnetic effect of the Mn^{2+} was calculated to a good approximation according to the following equations:

$$(\epsilon_{obs}^{Mn})_{Cr} = \left[\frac{\left(\frac{1}{T_1}\right)_{CrGTP}^{EMn} - \left(\frac{1}{T_1}\right)_{CrGTP}^{EMg}}{\left(\frac{1}{T_1}\right)_{CrGTP}^{Mn} - \left(\frac{1}{T_1}\right)_{CrGTP}^{Mg}}\right] \quad (11)$$

$$(\epsilon_{obs}^{Mn})_{Co} = \left[\frac{\left(\frac{1}{T_1}\right)_{CoGTP}^{EMn} - \left(\frac{1}{T_1}\right)_{CoGTP}^{EMg}}{\left(\frac{1}{T_1}\right)_{CoGTP}^{EMn} - \left(\frac{1}{T_1}\right)_{CoGTP}^{EMg}}\right] \quad (12)$$

where $(1/T_1)_{CrGTP}^{EMn}$ or $(1/T_1)_{CoGTP}^{EMn}$ is the measured relaxation rate of the system containing the enzyme, Mn^{2+}, Cr^{3+}−GTP, or Co^{3+}−GTP and $(1/T_1)_{CrGTP}^{EMg}$ or $(1/T_1)_{CoGTP}^{EMg}$ is the measured relaxation rate of the system containing the enzyme, Mg^{2+}, Cr^{3+}−GTP, or Co^{3+}−GTP. The nonenzymatic control systems are denoted by $(1/T_1)_{CrGTP}^{Mn}$ or $(1/T_1)_{CoGTP}^{Mn}$ and by $(1/T_1)_{CrGTP}^{Mg}$ or $(1/T_1)_{CoGTP}^{Mg}$.

From the $1/T_1$ values, the enhancement values $[(\epsilon_{obs}^{Mn})_{Cr}$ and $(\epsilon_{obs}^{Mn})_{Co}]$ in eqs 11 and 12 can be determined. The enhancement values can then be used to calculate $f(\tau_c)$ in eq 10. The values for τ_c for both the Cr^{3+} and Co^{3+} (paramagnetic and diamagnetic) complexes were then used to determine the distance between the two metals as shown in eq 13:

$$\frac{1}{\tau_c^{Cr}} - \frac{1}{\tau_c^{Co}} = \frac{2(\text{constants})}{15r^{6}}\tau_s^{Cr} \quad (13)$$

where the constants equal 5.63×10^{22} and τ_s^{Cr} is 2.3×10^{-10} s.

This same series of measurements, with the corresponding diamagnetic controls, and calculations were repeated to determine the distance between Mn^{2+} at site n_1 and Cr^{3+} at site n_2 in the $Mn^{2+}(n_1)$−PEPCK−$Cr^{3+}(n_2)$−GDP complex, and the distance between Cr^{3+} at site n_1 and Mn^{2+} at site n_2 in the $Cr^{3+}(n_1)$−PEPCK−$Mn^{2+}(n_2)$−GTP and $Cr^{3+}(n_1)$−PEPCK−$Mn^{2+}(n_2)$−GDP complexes.

^1H and ^{31}P Relaxation Rate Measurements. The relaxation rate experiments were performed on Varian Unity Plus 300 MHz and Varian VXR 500 MHz spectrometers. The effects of Mn^{2+} on $1/T_1$ and $1/T_2$ values of the trans and cis protons and the ^{31}P nucleus of PEP were measured. The T_1 measurements were made by the inversion recovery method (180°−τ−90°) (*31*, *32*) in the absence and in the presence of Mn^{2+}. For T_1 measurements, multiple scans were accumulated at each τ value. The number of scans depended upon the signal-to-noise ratio of the particular experiments. $1/T_1$ values were obtained from the best fit to a single-exponential decay.

The T_2 values were estimated from the line widths of the resonance signals with the equation

$$1/T_2 = \pi(\nu_{1/2} - B) \quad (14)$$

where $\nu_{1/2}$ is the spectral line width at half-height in hertz and B is the artificial line broadening due to the exponential multiplication of the FID prior to Fourier transformation of the spectrum. The value of B was usually 0.5 Hz.

The ^{1}H relaxation rates were determined at 300 and 500 MHz. The ^{31}P relaxation effects were determined at 121.5 and 202.5 MHz. The ^{1}H relaxation rates at 500 MHz were measured from ^{31}P-decoupled spectra. The ^{31}P relaxation rates were obtained from ^{1}H-decoupled spectra. All samples were run in 5 mm sample tubes with a final volume of 750 μL. Unless mentioned otherwise, the temperature was regulated at 21 ± 1 °C.

All of the relaxation rate experiments (^{1}H and ^{31}P) were performed under analogous experimental conditions. Solutions were prepared in 50 mM Tris-HC1 buffer (pD 7.4), which contained 100 mM KC1 in D_2O. In the absence of enzyme, the ligand concentration was approximately 10 mM for each of the experiments. The exact concentration was determined independently. The $1/T_1$ and $1/T_2$ values were measured as a function of increasing concentrations of $MnCl_2$. The experiments performed in the presence of enzyme were devised to maximize the distribution of Mn^{2+} into the $Co^{3+}(n_1)$−PEPCK−$Mn^{2+}(n_2)$−GDP−PEP complex. For the measurements of both ^{1}H and ^{31}P relaxation rates, the enzyme concentration was 100 μM and the PEP concentration was 10 mM. The Mn^{2+} concentration was varied from 0 to 4 μM. The observed $1/T_1$ values increased by a factor of 2−10 upon the addition of increasing amounts of Mn^{2+}. For each experiment that was performed, the distribution of Mn^{2+} was calculated on the basis of known dissociation constants for each complex (*7*). In each experiment performed in the presence of enzyme, >98% of the Mn^{2+} was calculated to be in the $Co^{3+}(n_1)$−PEPCK−$Mn^{2+}(n_2)$−GDP−PEP complex. To further verify the results of these calculations, several ^{1}H and ^{31}P experiments were performed at either two ligand concentrations or two enzyme concentrations. The normalized relaxation rates were virtually identical.

The relaxation rates, $1/T_1$ and $1/T_2$, were plotted as a function of Mn^{2+} concentration, and the paramagnetic contribution to the relaxation rates was calculated as the difference in relaxation rates due to Mn^{2+}. These values were normalized by the factor p, where $p = [Mn^{2+}]/[PEP]$, to yield values of $1/(pT_{1p})$ and $l/(pT_{2p})$. The normalized relaxation rates were assumed to be in fast exchange for initial analysis; thus, $1/(pT_{1p}) = 1/T_{1M}$, and $1/(pT_{2p}) = 1/T_{2M}$.

The correlation time, τ_c, for the electron−nuclear interaction was calculated for each of the binary and enzyme complexes that was evaluated. The correlation time, τ_c, was defined by eq 10. For the binary complexes, τ_c was assumed to be τ_r, the rotational correlation time. For the binary complexes, this value increases approximately 80% from the T_1 for $Mn(H_2O)_6$ (3×10^{-11} s) (*24*) when the $Mn(H_2O)_5$−ligand complex is formed. A value of 5.38×10^{-11} s was calculated for τ_c for the binary complexes on the basis of the increase in molecular weight.

Two separate methods were used to determine τ_c in the enzyme complexes. Both of these methods utilized the dipolar forms of the Solomon−Bloembergen equations (*26*, *27*). The abbreviated Solomon−Bloembergen equations (the scalar term has been ignored in these calculations) are represented by eqs 5 and 15:

$$\frac{1}{T_{2M}} = \frac{q[SS(S+1)\gamma^2 g^2 \beta^2]}{15r^6} \times \left(4\tau_c + \frac{3\tau_c}{1+\omega_I{}^2\tau_c{}^2} + \frac{7\tau_c}{1+\omega_s{}^2\tau_c{}^2}\right) \quad (15)$$

The above terms have been previously defined. A frequency dependence of $1/T_{1M}$ for the nucleus measured was used to calculate τ_c. Assuming τ_c is frequency-independent, eq 16

$$\frac{T_{1M(\nu_2)}}{T_{1M(\nu_1)}} = \frac{1+\omega_{I(\nu_2)}{}^2\tau_c{}^2}{1+\omega_{I(\nu_1)}{}^2\tau_c{}^2} \quad (16)$$

was used to calculate τ_c. Assuming a maximal frequency dependence of τ_c, eq 17 was used to calculate τ_c at ν_1 and ν_2:

$$\frac{T_{1M(\nu_2)}}{T_{1M(\nu_1)}} = \frac{1+\omega_{I(\nu_2)}{}^2(\nu_2/\nu_1)\tau_c{}^2}{1(\nu_2/\nu_1)^2+\omega_{I(\nu_1)}{}^2\tau_c{}^2} \quad (17)$$

The second method for calculating τ_c utilized the $(1/T_{2M})/(1/T_{1M})$ ratio. Assuming only dipolar contributions of Mn^{2+} to the relaxation rates, τ_c can be calculated from the following relationship:

$$\tau_c = \left[\frac{6\left(\frac{T_{1M}}{T_{2M}}\right) - 7}{4\omega_I{}^2}\right]^{1/2} \quad (18)$$

The longitudinal relaxation rates of the nuclei of a complexed ligand ($1/T_{1M}$) may be used in the Solomon−Bloembergen equations to calculate interatomic distances between the paramagnetic ion and the magnetic nuclei from the dipolar correlation time, τ_c. The equation is restricted by the limits of fast exchange ($pT_{1p} = T_{1M}$). For Mn^{2+}−^{1}H interactions in a 1:1 complex, the simplified form of eq 5 is

$$r(\text{Å}) = 812[T_{1M}f(\tau_c)]^{1/6} \quad (19)$$

and for Mn^{2+}−^{31}P interactions, the equation simplifies to

$$r(\text{Å}) = 601[T_{1M}f(\tau_c)]^{1/6} \quad (20)$$

The term $f(\tau_c)$ is the correlation function (eq 10). A more detailed description of the treatment of these data has been reviewed elsewhere (*19*).

A temperature dependence of the ^{31}P relaxation rates of PEP in the ternary complex was performed at 121.5 MHz. One sample contained 100 μM $Co^{3+}(n_1)$−PEPCK in the presence of 80 μM GDP and 10 mM PEP, and the other was the same but in the presence of 4 μM Mn^{2+}. Differences in relaxation rates between the Mn^{2+}-containing complex and the diamagnetic control were calculated to give values for the paramagnetic contribution to the relaxation rates. The temperature was varied by passing cooled nitrogen over a thermostated heating element before it arrived at the sample zone. The temperature of the sample within the core was measured directly by means of a thermocouple.

LysC Digestion of Apo- and $Co^{3+}(n_1)$−PEPCK−$Co^{3+}(n_2)$−GTP. ApoPEPCK and $Co^{3+}(n_1)$−PEPCK−$Co^{3+}(n_2)$−GTP

solutions were concentrated in 50 mM Tris-HCl (pH 7.4) to approximately 9 mg/mL using a mini-Amicon concentrator with a PM30 membrane. Urea (6 M) was added to the enzyme solutions, and the mixtures were incubated at 90 °C for 30 min. The $Co^{3+}(n_1)$−PEPCK−$Co^{3+}(n_2)$−GTP solution was then added to an Eppendorf tube containing Chelex-100 resin. The tube was gently shaken and quick-spun using a minicentrifuge to pellet the resin. The cobalt content was determined from the supernatant by AA. After heating, sufficient 25 mM Tris-HCl (pH 7.4) was added to the solutions to dilute the urea concentration to 2 M. LysC, at a 1:50 (w/w) ratio, was added. Nitrogen gas was blown over the solutions. The LysC digest mixtures were incubated at 37 °C for 24 h. After digestion, the $Co^{3+}(n_1)$−PEPCK−$Co^{3+}(n_2)$−GTP solution was treated with Chelex-100 as before to remove any free cobalt ions.

Separation of the Proteolytic Digests by Reverse-Phase HPLC. LysC peptides were separated on a C-18 reverse-phase Rainin Microsorb-MV (4.6 mm × 250 mm) column with a 300 Å pore size using a computer-assisted Waters 501 HPLC two-pump system equipped with a Waters 484 tunable absorbance detector and a Waters system interface module. Approximately 1 mg of digested protein was injected into the system. LysC peptides were eluted with the following gradient: 99.9% water with 0.1% trifluoroacetic acid for 10 min, 0 to 40% acetonitrile in 0.1% trifluoroacetic acid wash for 1 min, and 40 to 99.9% acetonitrile in 0.1% trifluoroacetic acid for 50 min, followed by a 99.9% acetonitrile in 0.1% trifluoroacetic acid wash for an additional 20 min. The flow rate was maintained at 0.8 mL/min throughout the entire run. Peptides were detected at 215 nm. One milliliter fractions were collected for the first hour. The cobalt content for each fraction was detected by AA.

Two cobalt-containing peptides were detected. The first cobalt-containing peptide was previously identified as the peptide associated with the n_1 metal site on PEPCK. The second cobalt-containing peptide was treated with 143 mM β-met and Chelex-100 to remove the cobalt that may interfere with peptide sequencing. The peptide buffer was then exchanged into distilled deionized water by running the sample through a 10 mL P6-DG column equilibrated in distilled deionized water. This process eliminated any contaminating primary amines that may interfere with amino acid composition analysis. The sample was submitted to the Bio-Core Facility at the University of Notre Dame, Department of Chemistry and Biochemistry, for amino acid composition and sequence analysis.

RESULTS

Presence of the Second Metal Site on PEPCK. The diamagnetic exchange-inert $Co^{3+}(n_1)$−PEPCK complex provides an excellent experimental tool for examining the role of the second metal in PEPCK activity. To investigate the role of the second metal, EPR and PRR titrations of Mn^{2+} binding to 100 μM Co^{3+}−PEPCK in the presence of 90 μM GTP or 80 μM GDP were performed. Unmodified PEPCK with GTP or GDP was used as a control. On the basis of the K_D values of 2 μM for the PEPCK−GTP complex (*5*) and 10 μM for the PEPCK−GDP complex (*7*), approximately 80−90% of the total nucleotide present was bound to PEPCK to form the respective binary complexes.

Table 1: Mn^{2+} Binding Constants for Various PEPCK Complexes

	PRR measurements		EPR measurements	
sample	n[a]	K_D (μM)	n[a]	K_D (μM)
apoPEPCK	0.95 ± 0.06	46.7 ± 5.1	1.02 ± 0.10	48.5 ± 6.2
PEPCK−PEP	0.98 ± 0.09	12.0 ± 4.7	1.08 ± 0.13	13.6 ± 6.2
PEPCK−GDP	1.77 ± 0.12	19.8 ± 5.6	1.79 ± 0.21	21.0 ± 3.3
PEPCK−GTP	1.88 ± 0.11	9.8 ± 3.0	1.94 ± 0.11	10.0 ± 1.8
Co^{3+}−PEPCK	0[b]	−	0[b]	−
Co^{3+}−PEPCK−PEP	0[b]	−	0[b]	−
Co^{3+}−PEPCK−GDP	0.79 ± 0.15	10.9 ± 0.9	0.81 ± 0.11	9.9 ± 0.3
Co^{3+}−PEPCK−GTP	0.86 ± 0.13	5.7 ± 0.4	0.91 ± 0.06	4.9 ± 0.3

[a] n represents the stoichiometry of Mn^{2+} to enzyme as determined from Scatchard analysis. Data were fit using EZ-Fit, version 2.02, by Perella Scientific Inc. (1989). [b] No measurable Mn^{2+} binding was observed for these samples.

As shown in Table 1, stoichiometry values increased from 1 to ∼2 mol of Mn^{2+} bound per mole of enzyme in the presence of GTP or GDP with a decrease in K_D values for Mn^{2+} to approximately 10−20 μM. This indicates that Mn^{2+}−GTP or Mn^{2+}−GDP interacts with the Mn^{2+}−PEPCK binary complex at the second metal site on PEPCK to form the bimetal complex. Although a stoichiometry of nearly 2 mol of Mn^{2+} bound per mole of apoenzyme was observed, the data can best be fit to a single K_D. No Mn^{2+} binding was observed for $Co^{3+}(n_1)$−PEPCK in the absence or presence of PEP. These results agree with previous observations that indicate Co^{3+} is at the n_1 site on PEPCK (*7*). Binding of Mn^{2+} to $Co^{3+}(n_1)$−PEPCK was observed only when GTP or GDP was present (Table 1), indicating that binding must be at the n_2 site of the enzyme. As determined from a Scatchard analysis (*22*) of both EPR and PRR data, approximately 1 mol of Mn^{2+} binds per mole of the $Co^{3+}(n_1)$−PEPCK−GTP or $Co^{3+}(n_1)$−PEPCK−GDP complexes. The K_D value for Mn^{2+} binding was approximately 5 μM for $Co^{3+}(n_1)$−PEPCK−$Mn^{2+}(n_2)$−GTP and 10 μM for $Co^{3+}(n_1)$−PEPCK−$Mn^{2+}(n_2)$−GDP. These values are significantly smaller than the K_D values for Mn^{2+} binding to free GTP (approximately 80 μM) or to free GDP (approximately 800 μM), suggesting that PEPCK provides ligands to the n_2 metal.

Substrate Binding to the $Co^{3+}(n_1)$−PEPCK−$Mn^{2+}(n_2)$−GTP and $Co^{3+}(n_1)$−PEPCK−$Mn^{2+}(n_2)$−GDP Complexes As Assessed by PRR Measurements. The interaction of PEP, OAA, and CO_2 (treated as HCO_3^-) with either $Co^{3+}(n_1)$−PEPCK−$Mn^{2+}(n_2)$−GTP or $Co^{3+}(n_1)$−PEPCK−$Mn^{2+}(n_2)$−GDP was investigated using PRR techniques. As shown in Figure 1A, the titration of $Co^{3+}(n_1)$−PEPCK−$Mn^{2+}(n_2)$−GDP with PEP results in a decrease in the observed enhancement, indicating the formation of a quinary $Co^{3+}(n_1)$−PEPCK−PEP−$Mn^{2+}(n_2)$−GDP complex. The data from several titration studies were evaluated by iterative computations to obtain values for K_3 and ϵ_t. The best fit to the data (<4% standard deviation) yields a dissociation constant (K_3) of 1.86 ± 0.07 μM for dissociation of PEP from $Co^{3+}(n_1)$−PEPCK−$Mn^{2+}(n_2)$−GDP and an enhancement (ϵ_t) of 3.25 ± 0.13. These results are summarized in Table 2. The dissociation constant of 1.86 μM for PEP is in good agreement with previous PRR studies of the $Mn^{2+}(n_1)$−PEPCK complex that gave a K_3 of 0.6 μM for PEP (*21*). The titration of PEP into $Co^{3+}(n_1)$−PEPCK−$Mn^{2+}(n_2)$−GTP did not change the relaxation rate over the concentration range of PEP (0−320 μM) that was examined.

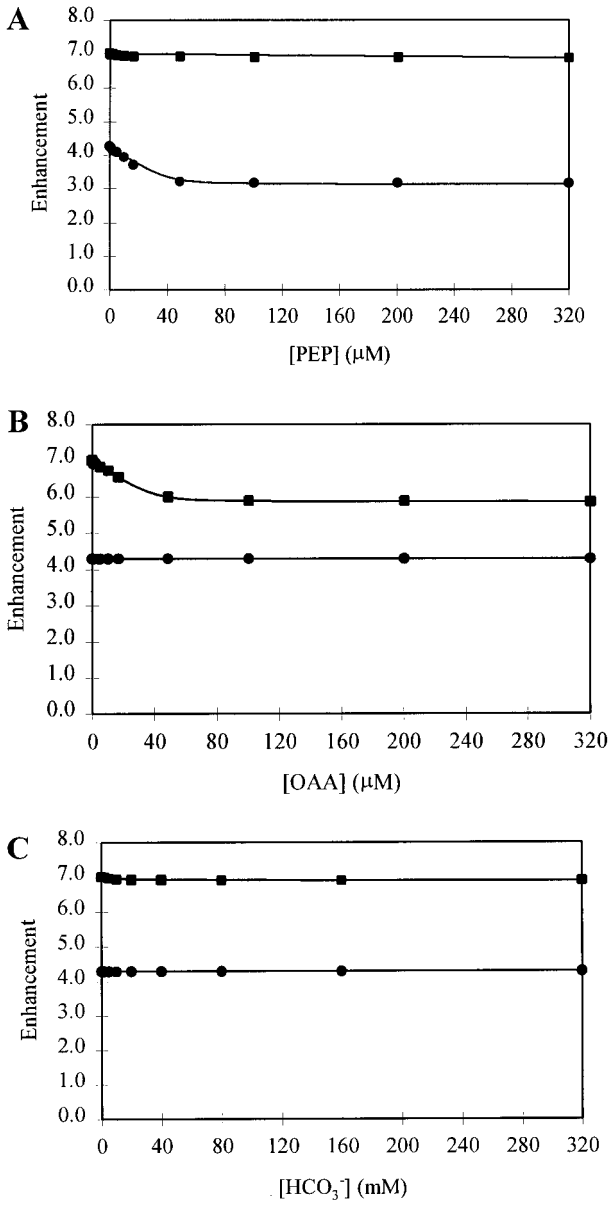

FIGURE 1: PRR titration of substrates into the $Co^{3+}(n_1)$−PEPCK−$Mn^{2+}(n_2)$−nucleotide complexes. (A) PRR titration of PEP into $Co^{3+}(n_1)$−PEPCK−$Mn^{2+}(n_2)$−GTP (■) or $Co^{3+}(n_1)$−PEPCK−$Mn^{2+}(n_2)$−GDP (●). (B) PRR titration of OAA into $Co^{3+}(n_1)$−PEPCK−$Mn^{2+}(n_2)$−GTP (■) or $Co^{3+}(n_1)$−PEPCK−$Mn^{2+}(n_2)$−GDP (●). (C) PRR titration of CO_2 (treated as HCO_3^-) into $Co^{3+}(n_1)$−PEPCK−$Mn^{2+}(n_2)$−GTP (■) or $Co^{3+}(n_1)$−PEPCK−$Mn^{2+}(n_2)$−GDP (●). The curves represent the best fits to the experimental data.

These results agree with fluorescence studies (not shown) where GTP was titrated into the $Co^{3+}(n_1)$−PEPCK−PEP complex. No change in PEPCK fluorescence was observed, indicating that GTP does not bind to the $Co^{3+}(n_1)$−PEPCK−PEP complex. It appears that PEPCK cannot accommodate both GTP and PEP at its active site. The γ-phosphate group of GTP and the phosphate moiety of PEP may occupy the same position at the active site of PEPCK, preventing both substrates from binding simultaneously.

The titration of $Co^{3+}(n_1)$−PEPCK−$Mn^{2+}(n_2)$−GTP with OAA (Figure 1B) results in a decrease in the observed enhancement, indicating the formation of a quinary $Co^{3+}(n_1)$−PEPCK−$Mn^{2+}(n_2)$−GTP−OAA complex. The results of the fits are given in Table 2. The results suggest that the interaction of OAA with $Co^{3+}(n_1)$−PEPCK−$Mn^{2+}(n_2)$−GTP affects the environment of the second metal. The quinary $Co^{3+}(n_1)$−PEPCK−$Mn^{2+}(n_2)$−GTP−OAA complex is catalytically active, with PEP, CO_2, and GDP being formed as products. The change in enhancement may reflect the formation of diphosphate nucleotide, GDP, from triphosphate nucleotide, GTP. GDP is proposed to be in a monodentate complex with the n_2 metal, whereas GTP is in a bidentate complex. The observed change in enhancement may indicate the exchange of ligands for the n_2 metal. The PRR titration of OAA into $Co^{3+}(n_1)$−PEPCK−$Mn^{2+}(n_2)$−GDP did not change the enhancement over the concentration range of OAA (0−320 μM) that was examined. This dead-end complex is not catalytically active; either OAA does not affect the environment of the n_2 metal, or the complex does not form.

The titration of the $Co^{3+}(n_1)$−PEPCK−$Mn^{2+}(n_2)$−GTP or $Co^{3+}(n_1)$−PEPCK−$Mn^{2+}(n_2)$−GDP complexes with HCO_3^- (CO_2 is the actual form of the substrate) did not change the enhancement over the concentration range of HCO_3^- (0−320 mM) that was examined (Figure 1C). HCO_3^- does not affect the environment of the n_2 metal.

Second Metal Hydration Number. The hydration number of the cation at the second metal site was determined using the $Co^{3+}(n_1)$−PEPCK−$Mn^{2+}(n_2)$−GTP and $Co^{3+}(n_1)$−PEPCK−$Mn^{2+}(n_2)$−GDP complexes. Measurements were taken for each protein−nucleotide−metal complex at two different enzyme concentrations (80 and 90 μM) and at five frequencies. Frequency-dependent data were fit utilizing a computer program to simulate the data as described in Materials and Methods.

Figure 2 shows the frequency dependence of pT_{1p} values for the $Co^{3+}(n_1)$−PEPCK−$Mn^{2+}(n_2)$−GTP and $Co^{3+}(n_1)$−PEPCK−$Mn^{2+}(n_2)$−GDP complexes. The normalized relaxation time shows a frequency dispersion. Table 3 lists the calculated values for several important parameters, including the hydration number, q, obtained from the generated fit and assuming that the metal-to-water proton distance is 2.87 Å. The hydration number for Mn^{2+} at site n_2 for the GTP complex is 0.56, and the value increases to 0.68 for the GDP complex. The nonintegral values calculated for q may be due to either the metal-bound water having only one proton in fast exchange, errors in the constants utilized, or collective uncertainties in the data fitting.

The apparent increase in q suggests that the number of protons in fast exchange increases for the GDP complex. This agrees with the metal−metal distance data (discussed below) that indicate a conformational change at the active site depending on whether the diphosphate or triphosphate nucleotide is bound. On the basis of these data, no more than one water molecule is associated with the second metal. Since Mn^{2+} prefers an octahedral geometry, the remaining five ligands must be provided by the enzyme and nucleotide.

Temperature Effect on the Observed $1/pT_{1p}$ Values of the $Co^{3+}(n_1)$−PEPCK−$Mn^{2+}(n_2)$−GTP and $Co^{3+}(n_1)$−PEPCK−$Mn^{2+}(n_2)$−GDP Complexes. The $1/pT_{1p}$ values of water protons in the $Co^{3+}(n_1)$−PEPCK−$Mn^{2+}(n_2)$−GTP and $Co^{3+}(n_1)$−PEPCK−$Mn^{2+}(n_2)$−GDP complexes were determined as a function of temperature over the range of 5−40 °C using PRR. The plots are linear with a positive slope, indicative of a fast chemical exchange. The activation energies, E_a, were calculated from the slope of the line. The E_a for the Co^{3+}-

Table 2: Binding Constants for Binding of Substrates to $Co^{3+}(n_1)$−PEPCK−$Mn^{2+}(n_2)$−GTP or −GDP As Determined by PRR[a]

PEPCK complex	substrate	K_3 (μM)	ϵ_t
$Co^{3+}(n_1)$−PEPCK−$Mn^{2+}(n_2)$−GDP	PEP	1.86 ± 0.07	3.25 ± 0.13
	OAA	NR[b]	NR[b]
	CO_2 (HCO_3^-)	NR[b]	NR[b]
$Co^{3+}(n_1)$−PEPCK−$Mn^{2+}(n_2)$−GTP	PEP	NR[b]	NR[b]
	OAA	1.93 ± 0.08	5.86 ± 0.23
	CO_2 (HCO_3^-)	NR[b]	NR[b]

[a] Substrates were titrated into $Co^{3+}(n_1)$−PEPCK−$Mn^{2+}(n_2)$−GTP or −GDP complexes, and enhancement values were measured as described in the text. [b] NR indicates that the addition of this substrate to the enzyme complex did not generate a PRR response.

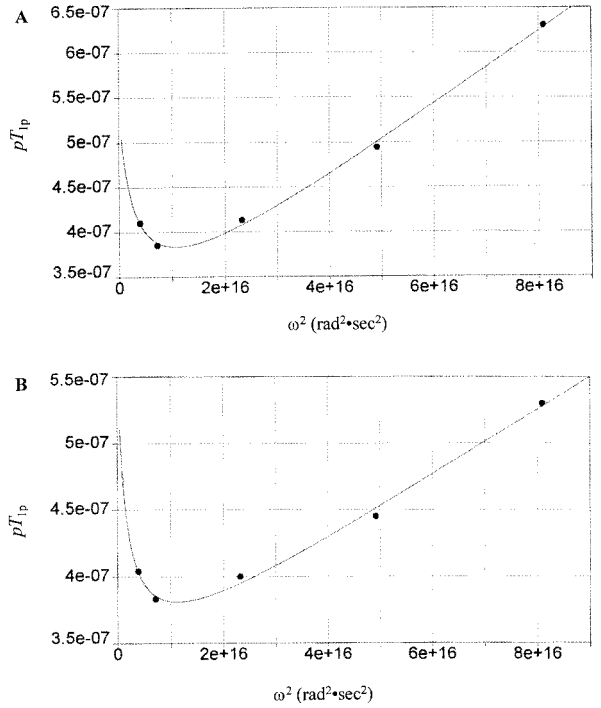

FIGURE 2: Frequency dependence of the PRR for the $Co^{3+}(n_1)$−PEPCK−$Mn^{2+}(n_2)$−nucleotide complexes. pT_{1p} is plotted vs the squared frequency (ω^2). (A) Frequency dependence for the $Co^{3+}(n_1)$−PEPCK−$Mn^{2+}(n_2)$−GTP complex. (B) Frequency dependence for the $Co^{3+}(n_1)$−PEPCK−$Mn^{2+}(n_2)$−GDP complex. pT_{1p} values were calculated for bound Mn^{2+} in each complex. The curves represent the best fits to the experimental data.

(n_1)−PEPCK−$Mn^{2+}(n_2)$−GTP complex is −5.85 kcal/mol. The E_a for the $Co^{3+}(n_1)$−PEPCK−$Mn^{2+}(n_2)$−GDP complex is −4.53 kcal/mol. These values differ considerably from those measured from the PRR temperature dependence of relaxation of water protons by the first metal site where the E_a is 1.7 to 2.3 kcal/mol (*32*) and in slow chemical exchange. The water molecules associated with the n_1 metal are proposed to interact with the phosphoryl group that undergoes transfer during catalysis (*5*, *6*).

Estimation of the Distance between the n_1 and n_2 Metal Sites on PEPCK. The distance between the n_1 metal and the n_2 metal in the $Cr^{3+}(n_1)$−PEPCK−$Mn^{2+}(n_2)$−GTP, $Cr^{3+}(n_1)$−PEPCK−$Mn^{2+}(n_2)$−GDP, $Mn^{2+}(n_1)$−PEPCK−$Cr^{3+}(n_2)$−GTP, and $Mn^{2+}(n_1)$−PEPCK−$Cr^{3+}(n_2)$−GDP complexes was estimated using PRR. Co^{3+}-labeled enzyme or Co^{3+}-labeled nucleotide or Mg^{2+}-bound enzyme or Mg^{2+}-labeled nucleotide was used as a diamagnetic control. All calculations were carried out as described by Gupta (*29*) and as outlined in Materials and Methods.

The measured $1/T_1$ values obtained from the PRR measurements for each bimetal complex system in the presence and absence of enzyme and for both the paramagnetic and diamagnetic metal ions allowed for the calculation of the ϵ_{obs} values [$(\epsilon_{obs}^{Mn})_{Cr}$ and $(\epsilon_{obs}^{Mn})_{Co}$] using eqs 11 and 12. From the ϵ_{obs} values, the $f(\tau_c)$ can be calculated from eq 9 and the values for τ_c can be calculated using eq 10. The differences in τ_c values obtained for the Cr^{3+} and Co^{3+} (paramagnetic and diamagnetic) complexes were used to calculate the distance, r, between the two metals using eq 13. The values for q, the hydration number, determined for the n_2 metal (see Table 3) were used in these calculations. Table 4 lists the ϵ_{obs}, τ_c, $\Delta\tau_c$, q, and r values.

An estimate of the correlation time, τ_c, affected by spin coupling of the two metal ions within the enzyme complex gives a value of 0.86 ns for the complexes with GTP and a value of 0.72 ns for the complexes with GDP. The metal−metal distance for the PEPCK complexes with GTP is approximately 8.3 Å, whereas the distance for the GDP complex is 9.2 Å (Table 4). The difference in the metal−metal distances for the two nucleotide−protein complexes suggests that a conformational change occurs during catalysis. This protein conformational change resulting in a 0.9 Å distance increase between the cations occurs at the PEPCK active site as GTP is converted to GDP.

Estimation of the Distance between the n_2 Metal and PEP on PEPCK. The effects of PEPCK-bound Mn^{2+} at site n_2 on the ^{31}P relaxation rates of PEP were measured at 121.5 and 202.5 MHz. The results of the Mn^{2+} titration on the $1/T_1$ and $1/T_2$ of ^{31}P for PEP at 121.5 MHz for the $Co^{3+}(n_1)$−PEPCK−GDP−PEP complex yield a linear response. Studies of the $Co^{3+}(n_1)$−PEPCK−GTP−PEP complex were not performed as fluorescence and PRR results demonstrate that this complex does not form. The $1/T_1$ and $1/T_2$ values for the ^{31}P nucleus increased by a factor of 2−10 upon the addition of up to 3.8 μM Mn^{2+} (data not shown). The data were normalized and are summarized in Table 5. The experiment was repeated at an approximately 25% greater enzyme concentration. The normalized relaxation rates from these experiments were nearly identical.

The effects of enzyme-bound Mn^{2+} on the ^1H relaxation rates for PEP were measured at 300 and 500 MHz. The $1/T_1$ values increased up to a factor of 10 as Mn^{2+} was added to a concentration of 3.8 μM. The data are summarized in Table 6. The normalized relaxation rates measured at 300 MHz for the PEP complex are enhanced over the values measured for the binary Mn^{2+}−ligand complexes.

To use the relaxation rate data in Tables 5 and 6 to calculate the Mn^{2+}−nuclear distance r from eqs 14 and 15, the ligands must be in fast exchange ($1/pT_{1p} = 1/T_{1M}$) and the correlation time, τ_c, must be known. It has previously been demonstrated (*19*) that when $1/pT_{2p}$ values are substantially larger than $1/pT_{1p}$ values, $1/pT_{1p}$ is often a measure

Table 3: Parameters Calculated from pT_{1p} vs $\omega_I{}^2$ [a]

sample	$1/pT_{1p}$ ($\times 10^{-6}$ s^{-1})[b]	τ_c (ns)	τ_v (ps)	B ($\times 10^{24}$)	q
$Co^{3+}(n_1)$−PEPCK−$Mn^{2+}(n_2)$−GTP	2.42	2.95	16.1	2.95	0.56
$Co^{3+}(n_1)$−PEPCK−$Mn^{2+}(n_2)$−GDP	2.50	2.57	22.4	2.57	0.68

[a] PRR measurements using $Co^{3+}(n_1)$−PEPCK−$Mn^{2+}(n_2)$−GTP or −GDP complexes were taken from the data presented in Figure 2. The results were fit to yield the pertinent parameters that are listed. [b] The $1/pT_{1p}$ values taken at 24.3 MHz were used for the calculation of the hydration number, q, for each complex.

Table 4: Metal−Metal Distances in the Bimetal M_1−PEPCK−M_2−Nucleotide Complexes[a]

sample	ϵ_{obs}	τ_c ($\times 10^{-10}$ s)	$1/\Delta\tau_c$ ($\times 10^7$ s)	q	r (Å)
$Mn^{2+}(n_1)$−PEPCK−$Cr^{3+}(n_2)$−GTP	2.64	8.63	3.96	0.56	8.3
$Mn^{2+}(n_1)$−PEPCK−$Co^{3+}(n_2)$−GTP	2.73	8.94			
$Cr^{3+}(n_1)$−PEPCK−$Mn^{2+}(n_2)$−GTP	2.63	8.60	3.99	0.56	8.3
$Co^{3+}(n_1)$−PEPCK−$Mn^{2+}(n_2)$−GTP	2.72	8.90			
$Mn^{2+}(n_1)$−PEPCK−$Cr^{3+}(n_2)$−GDP	2.67	7.15	2.11	0.68	9.2
$Mn^{2+}(n_1)$−PEPCK−$Co^{3+}(n_2)$−GDP	2.71	7.26			
$Cr^{3+}(n_1)$−PEPCK−$Mn^{2+}(n_2)$−GDP	2.68	7.18	2.10	0.68	9.2
$Co^{3+}(n_1)$−PEPCK−$Mn^{2+}(n_2)$−GDP	2.72	7.29			

[a] The distance between enzyme-bound metal (n_1) and the nucleotide-bound metal (n_2) were calculated using the PRR approach described by Gupta (*19*). Calculations for values of ϵ_{obs}, τ_c, $1/\Delta\tau_c$, q, and r are described in Materials and Methods.

Table 5: Normalized Effect of Mn^{2+} at Site n_2 of PEPCK on the ^{31}P of PEP in the $Co^{3+}(n_1)$−PEPCK−$Mn^{2+}(n_2)$−GDP−PEP Complex

nucleus	$1/pT_{1p}$ ($\times 10^3$ s^{-1})	$1/pT_{2p}$ ($\times 10^4$ s^{-1})	τ_c (ns)	$f(\tau_c)$ (ns)	r (Å)
^{31}P	4.68 ± 0.1[a]	1.31 ± 0.1[a]	2.05[c]	1.78	5.12 ± 0.12[c]
	4.20 ± 0.1[b]	−	0.42[d]	1.19	4.75 ± 0.15[d]

[a] Value measured at 121.5 MHz. [b] Value measured at 202.5 MHz. [c] Estimated from the ratio of $1/pT_{2p}$ to $1/pT_{1p}$ at 121.5 MHz. [d] Estimated from the ratio of $1/pT_{1p}$ at both frequencies.

Table 6: Normalized Effect of Mn^{2+} at Site n_2 of PEPCK on the Protons of PEP in the $Co^{3+}(n_1)$−PEPCK−$Mn^{2+}(n_2)$−GDP−PEP Complex

nucleus	$1/pT_{1p}$ ($\times 10^3$ s^{-1})	$1/pT_{2p}$ ($\times 10^3$ s^{-1})	τ_c (ns)	$f(\tau_c)$ (ns)	r (Å)
cis ^{1}H	2.60 ± 0.10[a]	8.69 ± 0.1[a]	0.96[c]	0.67	6.93 ± 0.20[c]
	0.29 ± 0.05[b]	−	0.36[d]	0.69	6.95 ± 0.17[d]
trans ^{1}H	1.53 ± 0.10[a]	6.19 ± 0.1[a]	1.08[c]	0.63	7.35 ± 0.11[c]
	0.19 ± 0.05[b]	−	0.31[d]	0.69	7.45 ± 0.10[d]

[a] Value measured at 300 MHz. [b] Value measured at 500 MHz. [c] Estimated from the ratio of $1/pT_{2p}$ to $1/pT_{1p}$ at 300 MHz. [d] Estimated from the ratio of $1/pT_{1p}$ at both frequencies.

of relaxation ($1/T_{1M}$) and is in the rapid exchange domain. Care must be taken with respect to the interpretation of the observed $1/T_{2p}$ values due to scalar coupling. Since $1/pT_{2p}$ values, measured for ^{31}P for PEP (Table 5), are much larger than the $1/pT_{1p}$ and $1/pT_{2p}$ values for the protons measured in the same complex and the relaxation rates are not identical (Table 6), these latter values reflect rapid exchange where $1/pT_{1p} = 1/T_{1M}$. The frequency dependence of $1/pT_{1p}$ for ^{31}P of PEP is also consistent with fast exchange. The correlation times for the Mn^{2+}−^{31}P interactions can therefore be calculated from the $1/T_{1M}$ values measured at 121.5 and 202.5 MHz (Table 5). Analogous calculations were performed for Mn^{2+}−^{1}H distances with $1/T_{1M}$ values measured at 300 and 500 MHz (Table 6). These calculations for the correlation time were performed assuming no frequency dependence of τ_c. The values for τ_c were also calculated from the $(1/T_{2M})/(1/T_{1M})$ ratios for each nucleus measured at 300 MHz for ^{1}H and 121.5 MHz for ^{31}P. The results of these calculations are summarized in Tables 5 and 6. The abnormally long values for τ_c calculated from $(1/T_{2M})/(1/T_{1M})$ ratio measurements of ^{31}P indicate that the T_{2M} values may contain scalar contributions to the relaxation. Ignoring the τ_c estimated from the $(1/pT_{2p})/(1/pT_{1p})$ ratio (see above) from ^{31}P studies, an average value for τ_c of 0.63 ± 0.32 ns for the Mn^{2+}−nuclear interactions on PEP was calculated.

The correlation times, calculated from the relaxation rates that were measured for each nucleus, were used to calculate the Mn^{2+}−nuclear distances, r. These calculations were performed with the simplified Solomon−Bloembergen equations, eqs 19 and 20 (*26*, *27*). The values for $f(\tau_c)$ and the values of $1/pT_{1p}$ were used to calculate r, the Mn^{2+}−nuclear distances. These values are summarized in Tables 5 and 6. The distance between Mn^{2+} at site n_2 on PEPCK and the cis and trans protons of PEP is 7.0 and 7.4 Å, respectively, while the distance between Mn^{2+} at site n_2 on PEPCK and ^{31}P of PEP is 4.8 Å. These distances are too great to suggest inner sphere coordination between Mn^{2+} at site n_2 and PEP. Mn^{2+} at site n_2 appears to form an outer sphere complex with ^{31}P of PEP. Lee et al. (*9*) showed that the n_2 metal interacts directly with the γ-phosphate group of GTP.

Temperature Effects of ^{31}P Relaxation Rates in the $Co^{3+}(n_1)$−PEPCK−PEP−$Mn^{2+}(n_2)$−GDP Complex. To confirm that the nuclei of PEP in the quinary $Co^{3+}(n_1)$−PEPCK−$Mn^{2+}(n_2)$−GDP−PEP complex are in fast exchange, the temperature dependence of the ^{31}P relaxation rate effects was measured. The temperature dependence of the Mn^{2+} effects on $1/pT_{1p}$ values of ^{31}P of PEP in the quinary PEPCK complex was measured at 5, 21, and 35 °C. The temperature dependence is linear with a positive slope, indicative of fast chemical exchange. The activation energy, E_a, calculated from the slope of the line for the $Co^{3+}(n_1)$−PEPCK−$Mn^{2+}(n_2)$−GDP complex is −0.38 kcal/mol. The diamagnetic control showed no change in $1/T_1$ or $1/T_2$ over the range that was observed. These results validate the earlier assumptions that the relaxation process is in fast exchange.

Characterization of the $Co^{3+}(n_1)$−PEPCK−$Mn^{2+}(n_2)$−GTP Complex. There have been several reported cases of modification of the first metal site on a protein by Co^{3+} (*7*, *11*, *33*−*38*) and Cr^{3+} (*10*, *11*, *37*−*40*), but there has been

Table 7: Kinetic Parameters of the PEPCK-Catalyzed Reaction of OAA to Pyruvate[a] for ApoPEPCK, $Co^{3+}(n_1)$−PEPCK, and $Co^{3+}(n_1)$−PEPCK−$Co^{3+}(n_2)$−GTP

sample	$K'_{m,OAA}$ (μM)	V_{max} (units/mg)	k_{cat}/K_a ($\times 10^5$ min^{-1} M^{-1})
apoPEPCK	111 ± 20	5.14 ± 0.16	34.3
$Co^{3+}(n_1)$−PEPCK	123 ± 11	1.03 ± 0.13	6.20
$Co^{3+}(n_1)$−PEPCK−$Co^{3+}(n_2)$−GTP[b]	131 ± 19	0.034 ± 0.007	0.19

[a] Kinetic assays were performed as described in the text. No β-met was present in the assay mix. [b] IDP was not required for this reaction.

no report in the literature of the modification of the second metal site on an enzyme.

The success of the modification of PEPCK with Co^{3+} (*7*) led to an investigation of the modification of the second metal site on PEPCK using similar techniques. The second metal of PEPCK is present only in the presence of nucleotide. An attempt was made to modify the second metal site of PEPCK using both the exchange-inert Co^{3+} and GTP to create a doubly labeled PEPCK complex. Kramer and Nowak (*12*) have shown that Co^{3+}−GTP was a competitive inhibitor of PEPCK. $Co^{3+}(n_1)$−PEPCK was incubated with Co^{2+} and GTP followed by the addition of 20 mM H_2O_2. After a period of 30 min, the solution was passed through a P6-DG column. The enzyme was assayed for protein concentration by Bradford assays and cobalt concentration by AA. A series of protein−nucleotide standards were measured at 260 nm. From this standard curve, the nucleotide concentration of the $Co^{3+}(n_1)$−PEPCK−$Co^{3+}(n_2)$−GTP complex was determined. It was found that a 2:1 stoichiometry of Co^{3+} to PEPCK and a 1:1 stoichiometry of GTP to PEPCK was found for this modified complex, indicating that a doubly labeled $Co^{3+}(n_1)$−PEPCK−$Co^{3+}(n_2)$−GTP complex had been formed. The Co^{3+} at the n_2 site appears to associate with both PEPCK and the nucleotide. This process modified the GTP site on PEPCK.

Mn^{2+} binding was assessed for the $Co^{3+}(n_1)$−PEPCK−$Co^{3+}(n_2)$−GTP complex using both PRR and EPR techniques. No Mn^{2+} binding to the doubly labeled complex was observed with either method, indicating that both metal sites on PEPCK are occupied by Co^{3+}.

GTP and GDP binding was assessed for the $Co^{3+}(n_1)$−PEPCK−$Co^{3+}(n_2)$−GTP complex using fluorescence. Previous studies have shown that GTP and GDP both quench PEPCK fluorescence, indicating binding of the nucleotides to PEPCK (*7*). Neither GTP nor GDP alters PEPCK fluorescence for the $Co^{3+}(n_1)$−PEPCK−$Co^{3+}(n_2)$−GTP complex, indicating that the added nucleotides do not bind to the doubly labeled enzyme. This indicates that the nucleotide position on the $Co^{3+}(n_1)$−PEPCK−$Co^{3+}(n_2)$−GTP complex is occupied. The Mn^{2+} and nucleotide binding studies show that this secondary modification appears to be specific for the n_2 site on PEPCK.

It was not possible to create a $Co^{3+}(n_1)$−PEPCK−$Co^{3+}(n_2)$−GDP doubly labeled complex using the same conditions for the GTP complex. Perhaps the lack of the γ-phosphoryl moiety on GDP prohibits the formation of such a stable exchange-inert complex. It is also possible that more stringent conditions are required to create the GDP doubly labeled complex. The concentration of H_2O_2 was increased to nearly 40 mM in the GDP incubation mixture; however, no changes were observed in the stoichiometry. At H_2O_2 concentrations greater than 40 mM, $Co^{3+}(n_1)$−PEPCK precipitates.

The $Co^{3+}(n_1)$−PEPCK−$Co^{3+}(n_2)$−GTP complex was inactive in both the forward (OAA to PEP) and reverse (PEP to OAA) PEPCK assays. The lack of activity for $Co^{3+}(n_1)$−PEPCK−$Co^{3+}(n_2)$−GTP contrasts with the activity observed for the $Co^{3+}(n_1)$−PEPCK and $Cr^{3+}(n_1)$−PEPCK complexes (*7*, *10*). This loss of activity is not surprising since GTP is now "permanently" associated with the enzyme. Freely associating nucleotide is required for turnover. Since no activity was observed by enzymatic assays for the formation of PEP, this suggests that the γ-phosphate of GTP in the $Co^{3+}(n_1)$−PEPCK−$Co^{3+}(n_2)$−GTP complex is associated with Co^{3+} at the n_2 site. If the γ-phosphate group were free, a single turnover might be expected. The enzymatic assay for PEPCK was developed to be sufficiently sensitive to observe a single turnover.

The lack of activity for $Co^{3+}(n_1)$−PEPCK−$Co^{3+}(n_2)$−GTP raised some concerns that the secondary modification damaged the enzyme even though treatment of $Co^{3+}(n_1)$−PEPCK with 20 mM H_2O_2 as a control did not result in any loss of activity or Co^{3+} label. For $Co^{3+}(n_1)$−PEPCK and $Cr^{3+}(n_1)$−PEPCK, the addition of β-met followed by gel filtration resulted in the loss of the cation with concomitant restoration of full PEPCK activity (*7*, *10*). Incubating $Co^{3+}(n_1)$−PEPCK−$Co^{3+}(n_2)$−GTP with 1.43 M β-met, 5 mM dithiothreitol, or 10 mM ascorbic acid for time periods of 5−120 min followed by gel filtration did not remove either Co^{3+} label as determined by AA or restore any PEPCK activity. The presence of GTP on the doubly labeled PEPCK may prevent the access of the reducing agents to the metal sites on the enzyme.

PEPCK catalyzes a second, experimentally irreversible decarboxylation of OAA to yield pyruvate (*13*):

$$\text{OAA} \xrightarrow{\text{NDP}} \text{pyruvate} + CO_2 \qquad (21)$$

This reaction requires a nucleotide diphosphate as a cofactor. The PEPCK-catalyzed reaction of OAA decarboxylation to pyruvate was assayed for the $Co^{3+}(n_1)$−PEPCK−$Co^{3+}(n_2)$−GTP complex. The PEPCK activity was coupled to lactate dehydrogenase, and the oxidation of NADH was spectrophotometrically characterized at 340 nm. PEPCK and $Co^{3+}(n_1)$−PEPCK catalyzed the conversion of OAA to pyruvate only in the presence of IDP. Table 7 lists the activities for this secondary PEPCK reaction and the K'_m values for OAA. The PEPCK-catalyzed reaction of OAA to pyruvate is approximately 70% as prevalent as the catalyzed reaction of PEP to OAA. $Co^{3+}(n_1)$−PEPCK has 18.1% of the activity of apoPEPCK for the ability to catalyze the conversion of OAA to pyruvate. This residual activity for $Co^{3+}(n_1)$−PEPCK corresponds to previously observed results that showed $Co^{3+}(n_1)$−PEPCK was 15−25% as active as unmodified PEPCK for the catalyzed reaction of PEP to OAA (*7*). The K'_m values for OAA were similar for both apoPEPCK and $Co^{3+}(n_1)$−PEPCK.

The $Co^{3+}(n_1)$−PEPCK−$Co^{3+}(n_2)$−GTP complex catalyzed the conversion of OAA to pyruvate, but did not require

the addition of the IDP cofactor. $Co^{3+}(n_1)$−PEPCK−$Co^{3+}(n_2)$−GTP was 0.6% as active as the unmodified enzyme (Table 7). Apparently, the Co^{3+}−GTP associated with the enzyme for this doubly labeled enzyme complex replaces the IDP function in the reaction.

$Co^{3+}(n_1)$−PEPCK−$Co^{3+}(n_2)$−GTP is only 3.3% as active as $Co^{3+}(n_1)$−PEPCK (in the presence of IDP) for the reaction of OAA to pyruvate (see Table 7). The low activity for $Co^{3+}(n_1)$−PEPCK−$Co^{3+}(n_2)$−GTP may be due to the presence of the triphosphate nucleotide rather than a diphosphate nucleotide. The $Co^{3+}(n_1)$−PEPCK−$Co^{3+}(n_2)$−GTP complex has a K'_m value for OAA similar to that for $Co^{3+}(n_1)$−PEPCK. This indicates that OAA associates similarly with both $Co^{3+}(n_1)$−PEPCK−$Co^{3+}(n_2)$−GTP and $Co^{3+}(n_1)$−PEPCK. It is possible that the $Co^{3+}(n_1)$−PEPCK−$Co^{3+}(n_2)$−GTP solution was contaminated with $Co^{3+}(n_1)$−PEPCK, which may account for the observed activity of the doubly labeled complex. However, if this were true, then one would also expect to observe approximately 3% activity in the normal PEPCK assay for this complex. This was not seen.

These results show that $Co^{3+}(n_1)$−PEPCK−$Co^{3+}(n_2)$−GTP is catalytically active and that $Co^{3+}(n_1)$−PEPCK was not damaged during the second modification process. PEPCK has been modified at both metal sites.

Separation of the Cobalt-Containing Peptides. The $Co^{3+}(n_1)$−PEPCK−$Co^{3+}(n_2)$−GTP complex was digested with LysC, and the digest was analyzed by RP-HPLC. The HPLC chromatographic profile is shown in Figure 3A. When this chromatogram is compared to that observed for the apo-PEPCK and $Co^{3+}(n_1)$−PEPCK digests (*7*), there appears to be a shift of a peak from 45 to 21 min, suggesting that the new peak at 21 min contains the second cobalt-labeled peptide. Previous work has shown that the cobalt-labeled peptide that corresponds to the n_1 site on PEPCK, after the identical treatment, elutes at 12 min (*7*). The same digest was run but monitored at an absorbance wavelength of 254 nm (Figure 3B). A peak at 21 min is the only one that is observed. This suggests that the nucleotide is associated with this peptide and that the new peak at 21 min is the second cobalt-labeled peptide. Figure 3C shows the cobalt content over the entire elution profile. Cobalt was detected in the peak that eluted at 4 min, which is the void volume peak and is indicative of some free cobalt. This was also observed in the chromatographic profile for $Co^{3+}(n_1)$−PEPCK (*7*). Cobalt was detected in the peaks at 12 and 21 min. The first cobalt-labeled peptide (12 min) was previously identified as the n_1 metal site (*7*). The peak at 21 min corresponds to the n_2 metal site.

The peak at 21 min was isolated. CE analysis of the second cobalt-labeled peptide showed a single peak at 19 min. Amino acid analysis and sequencing were performed on this peptide after cobalt (and GTP) removal by treatment with β-met followed by gel filtration. While β-met was unable to reduce the Co^{3+} label from the intact doubly labeled protein, it was able to reduce the cation from the peptide. This further suggests that the reducing reagents cannot access the active site of the doubly labeled PEPCK possibly due to the presence of the bulky nucleotide. Amino acid analysis (not shown) suggested that the peptide may be the region of Tyr57−Lys76. Electrospray mass spectroscopy gave a mass of 2388.0 Da for the peptide. This is within 0.2% of the calculated mass of 2393.8 Da for the region of Tyr57−Lys76.

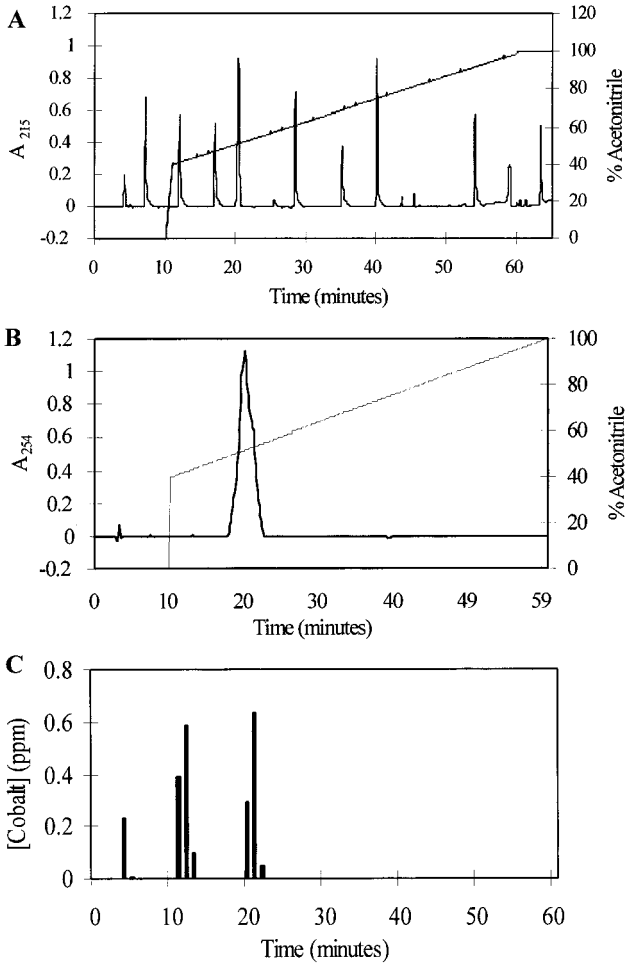

FIGURE 3: HPLC chromatographic profiles of $Co^{3+}(n_1)$−PEPCK−$Co^{3+}(n_2)$−GTP. (A) Co^{3+}−PEPCK−Co^{3+}−GTP was treated with 6 M urea and LysC (1:50 w/w) and incubated at 37 °C for 24 h. A reverse-phase C-18 HPLC column was used to separate the peptides. Peptides were eluted with the following gradient: 99.9% water with 0.1% trifluoroacetic acid for 10 min, 0 to 40% acetonitrile in 0.1% trifluoroacetic acid wash for 1 min, and 40 to 99.9% acetonitrile in 0.1% trifluoroacetic acid for 50 min, followed by a 99.9% acetonitrile in 0.1% trifluoroacetic acid wash for an additional 20 min. The absorbance was measured at 215 nm. (B) The same treatment as described for panel A but measured at 254 nm. (C) The cobalt content for the entire elution profile in panel A was assayed. The cobalt-containing fractions eluted between 5 and 6 min, between 11 and 13 min, and between 20 and 22 min.

Amino acid sequencing results are shown in Table 8. The sequencing results exactly match the sequence of the Tyr57−Ala71 region. The peptide must then be Tyr57−Lys76 where Lys56 is the preceding amino acid. This peptide is located near the N-terminus of the enzyme and close to the putative PEP binding site. Table 9 shows a sequence alignment of seven different species of PEPCK from the Tyr57−Lys76 region. This is a highly homologous region of PEPCK with 16 out of the 20 amino acids well conserved throughout the seven PEPCK sequences. This region contains one conserved aspartic acid residue, Asp69, one conserved glutamic acid residue, Glu74, and a well-conserved aspartic acid residue, Asp66 (using the avian liver numbering system). These are all feasible ligands to the metal. While Ser75 may also serve as a metal ligand, Vallee and Auld (*41*) found that aspartate predominates in catalytic metal sites where the binding frequency is as follows: Asp > His ≫ Glu ≫ Ser. It is less likely that serine is involved in metal chelation.

Table 8: Amino Acid Sequence Analysis of the Second Cobalt-Containing Peptide

cycle number	amino acid	peptide[a] (pmol of amino acid)	PEPCK Tyr57−Lys76
1	Tyr	9377.8	Tyr
2	Asp	6295.4	Asp
3	Asn	5103.7	Asn
4	Cys	−[b]	Cys
5	Trp	3371.5	Trp
6	Leu	3826.9	Leu
7	Ala	3420.1	Ala
8	Arg	4086.5	Arg
9	Thr	1015.3	Thr
10	Asp	757.3	Asp
11	Pro	209.0	Pro
12	Arg	167.7	Arg
13	Asp	25.6	Asp
14	Val	3.0	Val
15	Ala	0.3	Ala

[a] The second cobalt-containing peptide was sequenced at the Bio-Core Facility at the University of Notre Dame. [b] Sample not detected because neither the enzyme nor the peptide was modified to block free cysteines (e.g., with iodoacetate or *N*-ethylmaleimide) prior to sequencing. The chromatographic profile for this cycle was typical for unmodified cysteine.

Table 9: PEPCK Sequence Alignment[a]

Source	Position 57	60	65	70	75	76
Chicken mito.	**Y D N C W L A R T** D P R D V A R V E	**S K**
Chicken cyto.	**Y** E **N C W L A** L **T** N P R D V A R I E	**S K**
A. suum	**Y** K **N** N Y **L** C **R T** D P R D V A R V E	**S K**
H. contort.	**Y** E **N** N Y **L** C **R T** D P K D V A R V E	**S K**
Drosophila	**Y D N C W L A R T** N P A D V A R V E	S R
Rat	**Y D N C W L A** L **T** D P R D V A R I E	**S K**
Human	**Y D N C W L A** L **T** D P R D V A R I E	**S K**

[a] Comparison of the amino acid sequences of PEPCK from seven species between the region of residues 57−76 from avian liver mitochondrial PEPCK. The amino acid sequences of PEPCK from chicken liver mitochondria (Chicken mito.) (*2*), chicken liver cytosol (Chicken cyto.) (*44*), *Ascari suum* (*A. suum*) (*45*), *Haemonchus contortus* (*H. contort.*) (*46*), *Drosophila melanogaster* (*Drosophila*) (*47*), rat liver cytosol (Rat) (*48*), and human liver cytosol (Human) (*49*) are shown. Sequences were aligned to maximize the degree of overall identity between all of the sequences that are shown. The numbering system is based on the sequence of chicken mitochondrial PEPCK (*2*). The preceding amino acid in chicken mitochondrial PEPCK is Lys56. Residues that are identical among these enzymes and the chicken mitochondrial PEPCK are bold. The amino acids proposed to be involved in metal chelation are shaded.

DISCUSSION

Avian liver mitochondrial PEPCK requires two divalent metal ions for activity. One metal is associated with the enzyme at site n_1, while the other is complexed to the nucleotide at site n_2. Site n_2 is the metal−nucleotide complex that serves as the substrate. Mn^{2+} has been proposed as a regulator for this enzyme in vivo (*5*). PEPCK, in the presence or absence of PEP, binds one Mn^{2+} at site n_1, as determined by EPR and PRR (*20*), to form an enzyme−metal complex which is the active form of the enzyme. Kinetic and binding studies show that n_1 Mn^{2+} facilitates the interaction of PEP and nucleotide with the enzyme. The location of the n_1 metal binding site was recently identified as Asp295 and Asp296 (*7*). The role of the second metal is less clear. Lee et al. (*9*) proposed that the n_2 metal is in a β,γ-bidentate coordination with the nucleotide. Little else was known about the environment of the n_2 metal on PEPCK, including what, if any, protein ligands are provided by PEPCK. Several novel techniques were utilized to characterize the second metal site on PEPCK. The exchange-inert cations, Co^{3+} and Cr^{3+}, have been used to form cation−enzyme and cation−nucleotide complexes that proved to be valuable tools in mechanistic studies on a variety of enzymes. Both $Co^{3+}(n_1)$−PEPCK and $Cr^{3+}(n_1)$−PEPCK have been formed and characterized (*7*, *10*). $Co^{3+}(n_1)$−PEPCK and $Cr^{3+}(n_1)$−PEPCK provide excellent tools for the examination of the n_2 metal site on PEPCK without the problems of equilibrium metal binding to the n_1 metal site. Co^{3+}−GTP, Co^{3+}−GDP, Cr^{3+}−GTP, and Cr^{3+}−GDP have all been found to be competitive inhibitors of PEPCK (*12*). In the work presented here, we utilized the exchange-inert properties of these metal−protein and metal−nucleotide complexes to investigate the environment of the n_2 metal site on PEPCK.

EPR studies indicate that 2 mol of Mn^{2+} will bind to 1 mol of the PEPCK−nucleotide complex with K_D values of <20 μM (Table 1). No Mn^{2+} binding to $Co^{3+}(n_1)$−PEPCK was observed in the presence or absence of PEP. In the presence of nucleotide, 1 mol of Mn^{2+} binds per one mole of $Co^{3+}(n_1)$−PEPCK−nucleotide with a K_D value of <10 μM. These results demonstrate that a second metal will bind tightly to PEPCK but only in the presence of nucleotide. The low K_D values suggest that PEPCK provides ligands to the second metal.

A frequency dependence of PRR for the $Co^{3+}(n_1)$−PEPCK−$Mn^{2+}(n_2)$−GTP and $Co^{3+}(n_1)$−PEPCK−$Mn^{2+}(n_2)$−GDP complexes demonstrated a frequency dispersion of relaxation and indicates that no more than one water molecule associates with the n_2 metal. The normalized relaxation time is not linear with the square of the resonance frequency, and the τ_c value obtained from the data for the PEPCK complexes, approximately 3 ns, is consistent with the τ_s having a significant effect on the correlation time. These results are in good agreement with previous data (*23*). The hydration number, q, for Mn^{2+} in the $Co^{3+}(n_1)$−PEPCK−$Mn^{2+}(n_2)$−GTP complex is 0.56, whereas the value increases to 0.68 for Mn^{2+} in the $Co^{3+}(n_1)$−PEPCK−$Mn^{2+}(n_2)$−GDP complex (Table 3). The nonintegral values calculated for q appear to be due to the metal-bound water having only one proton in fast exchange. Temperature dependence studies revealed that the water protons are in fast exchange at the n_2 metal site. Only one proton associated with the n_2 metal-bound water molecule is proposed to be in fast exchange. On the assumption that the n_2 metal is six-coordinate, five remaining ligands to the metal are to be shared between the nucleotide and the enzyme. Lee et al. (*9*) reported that the n_2 metal is in a bidentate chelate with the nucleotide triphosphate and in a monodentate complex with the nucleotide diphosphate. These results do not preclude the possibility that the nucleotide offers two or more ligands to the n_2 metal. The remaining ligands are donated from the protein. If PEPCK provides three ligands to the second metal, this would account for the low hydration number and is consistent with the tight Mn^{2+} binding (K_D $= 5-10$ μM).

Using Cr^{3+}- and Co^{3+}-labeled PEPCK and nucleotide complexes, it was possible to use PRR to estimate the distance between the two metal sites. This method is based

upon spin−spin interactions among two paramagnetic cations in proximity to each other. A small decrease in enhancement effects is observed, giving rise to a τ_c for $Mn^{2+}-H_2O$ of 0.69 ns.

The distance between the two metals in the $Co^{3+}(n_1)$−PEPCK−$Mn^{2+}(n_2)$−GTP complex is estimated to be 8.3 Å, and the distance between the two metals in the $Co^{3+}(n_1)$−PEPCK−$Mn^{2+}(n_2)$−GDP complex is estimated to be 9.2 Å (Table 4). Lee and Nowak (*5*) showed that the phosphoryl groups of the nucleotide are approximately 6−7 Å from the n_1 metal. The distance from the phosphoryl groups of the nucleotide to the site n_2 metal should be approximately 3 Å, the distance expected for direct coordination. If the distance between the metals and the phosphate groups is linear, as much as 10 Å could separate the two metals. The values of 8.3−9.2 Å are in agreement with this maximum value.

The advantage of using the PRR technique as opposed to EPR to determine metal−metal distance is that a high concentration of enzyme is not required for the PRR measurements. For all experiments carried out via PRR techniques, we used 50 μM PEPCK. EPR experiments require enzyme concentrations of 700−1000 μM. This presents a solubility problem for PEPCK since the enzyme is unstable to precipitation at concentrations greater than 400 μM. While it may be possible to increase the PEPCK solubility via addition of a detergent, insufficient information is known concerning PEPCK and metal solubility under such conditions. These requirements make the EPR experiment less feasible.

The metal−metal distance appears to increase 0.9 Å for the GDP complex as compared to that for the GTP complex, suggesting a change in enzyme conformation relative to the movement of substrates during catalysis. The change in cation distances qualitatively agrees with the values of q that were determined (Table 3) that show an increase in the hydration number from 0.56 to 0.68 for Mn^{2+} in the GTP complex as compared to the GDP complex. The increase in the q value for the GDP complex suggests that both protons of the water bound at metal n_2 may approach fast exchange. In the determination of the metal−metal distances, r, and in the hydration number, q, small effects are observed and multiple-parameter fits used to analyze the data, respectively. The absolute values for r and q should thus be interpreted with care. The change in metal−metal distance and the q values suggests a change in the catalytic site as GDP is converted to GTP. The presence of GTP may decrease the size of the active site of PEPCK into a tighter conformation, while GDP increases the size of the active site. This "closing" and "opening" of the active site may assist in the catalytic process and in product release.

^{31}P NMR studies revealed that the phosphorus atom of PEP is approximately 4.7 Å from the n_2 metal in the $Co^{3+}(n_1)$−PEPCK−$Mn^{2+}(n_2)$−GDP−PEP quinary complex, indicating that the phosphate moiety of PEP is near but not in direct coordination with the n_2 metal. ^{1}H NMR studies revealed that the cis and trans protons of PEP are approximately 7.0 and 7.4 Å from the n_2 metal, respectively. These results are also consistent with PEP being in a second sphere coordination to the n_2 metal. This is similar to the conformation of PEP relative to the n_2 cation in pyruvate kinase (*42*).

The second sphere coordination of the phosphate group of PEP to the n_2 metal agrees with this "open" active site conformation for the GDP complex. During catalysis as GDP is converted to GTP, it is proposed that the active site "closes", allowing the phosphoryl group of PEP to migrate to the β-phosphate of GDP and directly bind with the n_2 metal in a first sphere complex. This proposal would agree with previous studies that suggest that the n_2 metal is in direct coordination with the γ-phosphate group of GTP (*9*).

The protein ligands for the n_2 metal were determined using the novel technique of creating a doubly labeled $Co^{3+}(n_1)$−PEPCK−$Co^{3+}(n_2)$−GTP complex. Treating $Co^{3+}(n_1)$−PEPCK with Co^{2+}, GTP, and H_2O_2 created a $Co^{3+}(n_1)$−PEPCK−$Co^{3+}(n_2)$−GTP complex. $Co^{3+}(n_1)$−PEPCK−$Co^{3+}(n_2)$−GTP is inactive for the standard PEPCK reactions. This complex does catalyze the conversion of OAA to pyruvate. This is the first time that such a modification of the second metal site on an enzyme has been reported. PEPCK appears to be very stable toward the oxidative treatment required for the double label.

The $Co^{3+}(n_1)$−PEPCK−$Co^{3+}(n_2)$−GTP complex was digested by LysC, and the cobalt-containing peptides were purified using reverse-phase HPLC. The LysC digest produced two pure peptides that contained cobalt. The first cobalt-labeled peptide at 12 min has previously been identified as the n_1 metal site. Mass, amino acid composition, and sequence analyses of the second cobalt-labeled peptide identified the peptide as the segment of residues Tyr57−Lys76. This highly conserved region is located near the N-terminus of PEPCK and is near the putative PEP binding region. Asp66, Asp69, and Glu74 (using the avian liver numbering system) appear to be the feasible metal ligands in this region. Future three-dimensional structure analysis of the avian liver mitochondrial PEPCK may identify the remaining metal ligands, if any.

It appears that all of the ligands to the second metal are oxygen. A limitation of Co^{3+}−protein modification is that stabilization of a Co^{3+} complex requires careful regulation of the coordination environment. A set of six ligands with sufficient field strength (ligands relatively high in the electrochemical series) must be provided. It is possible to produce a $Co^{III}(H_2O)_6^{3+}$ complex electrochemically, but it is unstable. A $Co^{III}(NH_3)_6^{3+}$ complex is very stable to reduction since ammonia is considerably higher than water in the electrochemical series (*43*). The apparent lack of nitrogen ligands for the second metal would explain the instability of the $Co^{3+}(n_1)$−PEPCK−$Co^{3+}(n_2)$−GTP complex, which precipitates after 24 h at 4 °C. It appears that Mn^{2+} is the best metal at the n_2 metal site (*7*, *20*). Mn^{2+} has a strong preference for oxygen ligands and may explain why only oxygen ligands were found for the n_2 metal.

Figure 4 presents a visual summary of all the information learned about the second metal site of avian liver PEPCK. This scheme is based on studies presented within this paper and previous structural studies (*5*−*7*). This information, combined with the previously determined structural data, provides a three-dimensional view of the putative active site structure of PEPCK. The role of the second metal appears to be as an acceptor of the phosphoryl group that undergoes transfer during catalysis. The n_2 metal facilitates the transition of GDP to GTP which "closes" the active site. In the reverse direction, the n_2 metal appears to move away from the active

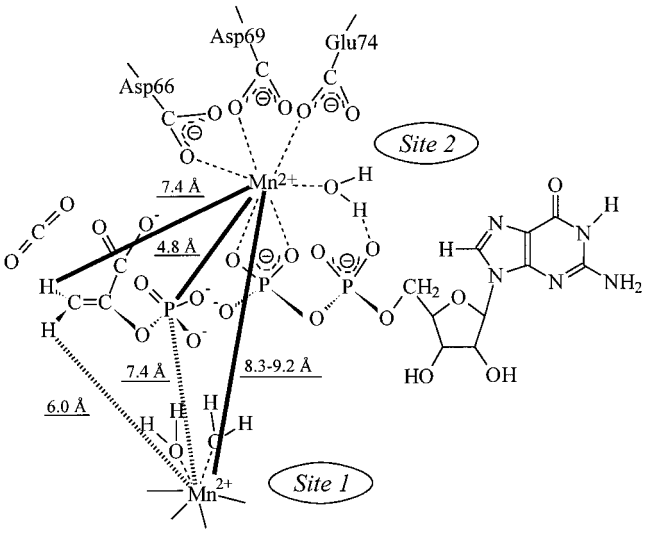

FIGURE 4: Revised active site scheme of avian liver mitochondrial PEPCK focusing on the second metal site of PEPCK. This scheme is based on studies presented within this paper and previous structural studies (*5*, *6*). The distance from the metal centers to only one of the protons of PEP is shown for clarity.

site while exchanging its ligands. This movement allows for a greater mobility at the active site, perhaps promoting product release.

In conclusion, the Co^{3+} and Cr^{3+} derivatives of PEPCK were used to characterize the structure and roles of the metal binding sites of PEPCK. These probes have allowed for the identification of the metal ligands at each site, and the characterization of the metal environments and the distances between the metals and substrates. In the absence of a three-dimensional structure for avian liver PEPCK, this information provides a great amount of knowledge about the active site of PEPCK.

ACKNOWLEDGMENT

We express our appreciation for the assistance of Don Schifferl in optimizing the EPR and PRR spectrometers, to Dr. Bakshy Chibber and Kay Finn in the Bio-Core Facility for obtaining amino acid sequence data, to Dr. Bill Boggess in the Mass Spectroscopy Facility for obtaining mass spectroscopy data, to Romeo and Delia Resiga for writing PRRFIT, and to Todd Holyoak and Michael Buening for writing FREQ.

REFERENCES

1. Utter, M. F., and Kurahashi, K. (1953) *J. Am. Chem. Soc. 75*, 258.
2. Weldon, S. L., Rando, A., Matathias, A. S., Hod, Y., Kalonick, P. A., Savon, S., Cook, J. S., and Hanson, R. W. (1990) *J. Biol. Chem. 265*, 7308−7317.
3. Matte, A., Goldie, H., Sweet, R. M., and Delbaere, L. T. J. (1996) *J. Mol. Biol. 256*, 126−143.
4. Lee, M. H., Hebda, C. A., and Nowak, T. (1981) *J. Biol. Chem. 256*, 12793−12801.
5. Lee, M. H., and Nowak, T. (1984) *Biochemistry 23*, 6506−6513.
6. Duffy, T. H., and Nowak, T. (1985) *Biochemistry 24*, 1152−1160.
7. Hlavaty, J. J., and Nowak, T. (1997) *Biochemistry 36*, 3389−3403.
8. Hlavaty, J. J., and Nowak, T. (1997) *Biochemistry 36*, 15515−15525.
9. Lee, M. H., Goody, R. S., and Nowak, T. (1985) *Biochemistry 24*, 7594−7602.
10. Hlavaty, J. J., and Nowak, T. (1998) *Biochemistry 37*, 8061−8070.
11. Balakrishnan, M. S., and Villafranca, J. J. (1979) *Biochemistry 18*, 1546−1551.
12. Kramer, P., and Nowak, T. (1988) *J. Inorg. Biochem. 32*, 135−151.
13. Noce, P., and Utter, M. F. (1975) *J. Biol. Chem. 250*, 9099−9105.
14. Hebda, C. A., and Nowak, T. (1982) *J. Biol. Chem. 257*, 5503−5514.
15. Cornelius, R. D., Hart, P. A., and Cleland, W. W. (1977) *Inorg. Chem. 16*, 2799−2805.
16. Gupta, R. K., Fung, C. H., and Mildvan, A. S. (1976) *J. Biol. Chem. 251*, 2421−2430.
17. DePamphilis, M. L., and Cleland, W. W. (1973) *Biochemistry 12*, 3714−3724.
18. Danenberg, K. D., and Cleland, W. W. (1975) *Biochemistry 14*, 28−39.
19. Carr, H. Y., and Purcell, E. M. (1954) *Phys. Rev. 94*, 630−639.
20. Nowak, T. (1981) Nuclear Relaxation Studies of Ligand-Exchange Interactions, in *Spectroscopy in Biochemistry* (Bell, J. E., Ed.) Vol. II, pp 109−135, CRC Press, Boca Raton, FL.
21. Hebda, C. A., and Nowak, T. (1982) *J. Biol. Chem. 257*, 5515−5522.
22. Scatchard, G. (1949) *Ann. N.Y. Acad. Sci. 51*, 660−672.
23. Hwang, S. H., and Nowak, T. (1989) *Arch. Biochem. Biophys. 269*, 646−663.
24. Bloembergen, N., and Morgan, L. O. (1961) *J. Chem. Phys. 34*, 842−850.
25. Swift, T. J., and Connick, R. E. (1962) *J. Chem. Phys. 37*, 307−310.
26. Solomon, I. (1955) *Phys. Rev. 99*, 559−565.
27. Solomon, I., and Bloembergen, N. (1956) *J. Chem. Phys. 25*, 261−266.
28. Fersht, A. (1985) The Three-Dimensional Structure of Enzymes, in *Enzyme Structure and Mechanism*, pp 1−46, W. H. Freeman and Co., New York.
29. Gupta, R. K. (1977) *J. Biol. Chem. 252*, 5183−5185.
30. Abragam, A. (1961) *The Principles of Nuclear Magnetism*, Chapter VIII, Clarendon Press, Oxford, U.K.
31. Vold, R. L., Waugh, J. S., Klein, M. P., and Phelps, D. E. (1968) *J. Chem. Phys. 48*, 3831−3832.
32. Allerhand, A., Doddrell, D., and Komoroski, R. (1971) *J. Chem. Phys. 55*, 189−197.
33. Kang, E. P., and Storm, C. B. (1972) *Biochem. Biophys. Res. Commun. 49*, 621−625.
34. Shinar, H., and Navon, G. (1974) *Biochim. Biophys. Acta 334*, 471−475.
35. Anderson, R. D., and Vallee, B. L. (1975) *Proc. Natl. Acad. Sci. U.S.A. 72*, 394−397.
36. Ryzewski, C., and Takahashi, M. T. (1975) *Biochemistry 14*, 4482−4486.
37. Miziorko, H. M., Behnke, C. E., and Houkom, E. C. (1982) *Biochemistry 21*, 6669−6674.
38. Lee, M. H. (1988) Ph.D. Dissertation, University of Notre Dame, Notre Dame, IN.
39. Kowalsky, A. (1969) *J. Biol. Chem. 244*, 6619−6625.
40. Pereira, M. A. P. (1990) Ph.D. Dissertation, University of Notre Dame, Notre Dame, IN.
41. Vallee, B. L., and Auld, D. S. (1993) *Biochemistry 32*, 6493−6500.
42. Gupta, R. K., and Benkovic, J. L. (1978) *J. Biol. Chem. 253*, 8878−8886.
43. Cotton, F. A., and Wilkinson, G. (1972) *Advanced Inorganic Chemistry: A Comprehensive Text*, 3rd ed., p 836, John Wiley & Sons, New York.
44. Cook, J. S., Weldon, S. L., Garcia-Ruiz, J. P., Hod, J., and

Hanson, R. W. (1986) *Proc. Natl. Acad. Sci. U.S.A. 83*, 7583−7587.
45. Geary, T. G., Winterwood, C. A., and Alexander-Bowman, S. J. (1993) *Exp. Parasitol. 77*, 155.
46. Klein, R. D., Winterwood, C. A., Hatzenbuhler, N. T., Shea, M. H., Favreau, M. A., Nulf, S. C., and Geary, T. G. (1992) *Mol. Biochem. Parasitol. 50*, 285−294.
47. Gundelfinger, E. B., Hermanns-Bergmeyer, J., Grenningloh, G., and Zopf, D. (1987) *Nucleic Acids Res. 15*, 6745.
48. Beale, E. G., Chrapkiewicz, M. B., Scoble, H. A., Metz, R. J., Quick, D. P., Noble, R. L., Donelson, J. E., Biemann, K., and Granner, D. K. (1985) *J. Biol. Chem. 260*, 10748−10760.
49. Ting, C. N., Burgess, D. L., Chamberlain, J. S., Keith, T. P., Falls, K., and Meisler, M. H. (1993) *Genomics 16*, 698−706.

BI991692A